

THESIS

COMPARISON OF DESIGN AND IMPLEMENTATION OF HYBRID SYSTEMS IN
PROTOTYPE VEHICLES

Submitted by

Benjamin Mckenney

Department of Mechanical Engineering

In partial fulfillment of the requirements

For the Degree of Master of Science

Colorado State University

Fort Collins, Colorado

Summer 2021

Master's Committee:

Advisor: Jason Quinn

Thomas Bradley

Brett Windom

Copyright by Benjamin Mckenney 2021
All Rights Reserved

ABSTRACT

COMPARISON OF DESIGN AND IMPLEMENTATION OF HYBRID SYSTEMS IN PROTOTYPE VEHICLES

With the continual increased concern with vehicle emissions, the automotive industry is focused on the advancement of new technology to reduce fuel consumption and curb emissions. The Colorado State University (CSU) Vehicle Innovation Team (VIT) has recently constructed two separate vehicle prototypes that utilize state of the art automotive technology for the purpose of furthering automotive research, specifically in the area of new controls techniques. The focus of these two projects have been on the integration of hybrid powertrains into traditional combustion engine driven vehicles. The vision, scope, and overall goals of each research project vary drastically, and thus the design choices vary as well. The contents of this paper will focus on the two separate hybrid vehicle projects and seek to capture the design and integration decisions that were made and provide insight and reasoning as to why the choices were made.

This process first begins with the background and scope of each project, which lays the groundwork for the design requirements that will drive each of the vehicle's overall architecture, design, function, and performance. Once these design requirements are understood, the component selection process is then examined for each vehicle. Fabrication and integration of the hybrid powertrain within the vehicle is also explored in a similar manner, in which the techniques and methodologies give an insight into the prototyping process. Throughout the sections the two different vehicle projects will be compared to one another and the differences

are discussed in detail as it pertains to the design requirements of each project. Finally, the testing procedures as well as results from the hybrid systems are presented.

ACKNOWLEDGMENTS

I would like to thank my advisors Dr. Thomas Bradley, Dr. Jason Quinn, and Dr. Brett Windom for their dedication, insight, and support with my thesis, as well as giving me the opportunity to continue my education in such a great group that is working on interesting and exciting projects. I would also like to thank all the professors who I have learned so much from at CSU, as well as all my teachers throughout my years of education that have fostered a great learning environment and inspired me to continue my education in STEM. I would also like to acknowledge the numerous project sponsors who have provided countless hours of time, parts, and money that were vital to the success of these projects.

Lastly, I would like to thank my family and friends for the continued love, support, and encouragement throughout every step of my career. Without the generous help from all these people this work would not have been possible.

TABLE OF CONTENTS

ABSTRACT.....	ii
ACKNOWLEDGMENTS	iv
LIST OF FIGURES	vii
Chapter 1: Introduction	1
1.1 Background.....	3
1.1.1 EcoCAR Mobility Challenge	3
1.1.2 Toyota Tacoma Test Vehicle Platform	4
1.2 Parameters that Effect Fuel Economy.....	4
1.3 Predictive Acceleration Events	5
1.4 Novel Contributions.....	6
Chapter 2: Design Criteria Comparisons	8
2.1 Autonomie Modeling.....	10
2.2 Vehicle Architectures.....	10
Chapter 3: Component Selection	15
3.1 Electric Motor	15
3.2 Inverter/ Electric Motor Controller	16
3.3 Energy Storage System.....	17
3.4 Internal Combustion Engine and Transmission	21
3.5 AC-DC Charger	22
Chapter 4: Development and Integration.....	24
4.1 Energy Storage System Enclosure	24
4.2 Battery Management System	31
4.3 High Voltage Wiring.....	34
4.3.1 Contactor Box and High Voltage Distribution box.....	38
4.4 High Voltage Charging	46
4.5 Low Voltage Wiring	48
4.5.1 Emergency Disconnect Switch	49
4.5.2 Wire Selection.....	50
4.5.3 Low Voltage Wire Preparations.....	52
4.6 Powertrain.....	53

4.7 Control System Integration	55
4.8 Human Machine Interface.....	56
4.9 Cooling System.....	60
Chapter 5: Fabrication Methodology	64
Chapter 6: Testing and Results	66
Chapter 7: Discussion	71
Chapter 8: Conclusion.....	72
References.....	74
Appendix.....	77
Pre-Charge Resistor Calculation MATLAB Script.....	77
Battery Management System Parameters	78
List of Abbreviations	79

LIST OF FIGURES

<i>Figure 1: TVP architecture diagram</i>	<i>12</i>
<i>Figure 2: Blazer architecture diagram</i>	<i>14</i>
<i>Figure 3: ThunderSky Winston LiFeYPO4 40 Ah battery</i>	<i>19</i>
<i>Figure 4: Elithion cell balancing board</i>	<i>20</i>
<i>Figure 5: HEV 4 installed in the rear spare tire well of the Blazer (APM not shown).....</i>	<i>25</i>
<i>Figure 6: Inverter installed into the rear spare tire well of the Blazer as seen from the underside of the vehicle</i>	<i>26</i>
<i>Figure 7: Battery box CAD renderings showing the components and frame, with and without the side panels and clear plastic lid</i>	<i>27</i>
<i>Figure 8: Manual Service Disconnect inserted into the receptacle on the TVP</i>	<i>28</i>
<i>Figure 9: Battery tray before installation</i>	<i>28</i>
<i>Figure 10: Welded battery enclosure frame with all 102 battery modules installed</i>	<i>30</i>
<i>Figure 11: Battery box installed in the bed of the Tacoma with the protective plastic lid shut</i>	<i>30</i>
<i>Figure 12: TVP high voltage wiring diagram</i>	<i>34</i>
<i>Figure 13: TVP high voltage battery routing diagram</i>	<i>35</i>
<i>Figure 14: High voltage connection protected via a washdown enclosure for the TVP</i>	<i>37</i>
<i>Figure 15: TVP contactor box wiring diagram</i>	<i>39</i>
<i>Figure 16: Pre-Charge resistor charging characteristics for TVP high voltage DC bus</i>	<i>43</i>
<i>Figure 17: High voltage junction box.....</i>	<i>45</i>
<i>Figure 18: TVP EVSE plug with connection callouts</i>	<i>47</i>
<i>Figure 19: Emergency disconnect switch installed on the rear bumper.....</i>	<i>49</i>
<i>Figure 20: Blazer rear subframe with Magna eRAD installed.....</i>	<i>54</i>
<i>Figure 21: YASA P400 Installed on the Tacoma Transmission (left) and Transmission/ EM System Installed on Vehicle (right)</i>	<i>55</i>
<i>Figure 22: Electric motor, transmission, and propulsion shaft installed in vehicle.....</i>	<i>55</i>
<i>Figure 23: CAD Model of Prototype Haptic Feedback System Housing Bottom view (left) and Top View (right) With Mockup Seat Belt Shown in Black.....</i>	<i>57</i>
<i>Figure 24: Haptic feedback system shown installed on the seatbelt with the top view (left) showing the connecting wires and the bottom view (right) showing the haptic motors.....</i>	<i>58</i>
<i>Figure 25: CAD model of the battery gauge (left) and 3D printed part with the battery gauge installed on the dashboard along with the PAE switches, EDS, and gateway power switch(right)</i>	<i>59</i>
<i>Figure 26: Contactor control switches CAD model mount (left) and 3D printed part installed in the vehicle</i>	<i>60</i>
<i>Figure 27: Blazer cooling loop diagram</i>	<i>61</i>
<i>Figure 28: TVP antifreeze reservoir mount with battery box rear mounting holes shown</i>	<i>63</i>
<i>Figure 29: CAN gateway mount CAD (left) and 3D printed part with the gateway installed (right)</i>	<i>65</i>
<i>Figure 30: Transmission tunnel hole with acrylic cover</i>	<i>65</i>
<i>Figure 31: High voltage DC bus current and voltage</i>	<i>67</i>
<i>Figure 32: Engine and electric motor torque for 90% ICE 10% EM torque split</i>	<i>68</i>

Figure 33: Torque commanded and actual torque from the electric motor 69
Figure 34: High voltage wire temperature 70

Chapter 1: Introduction

Since the mid-19th century, the industrializing of society has led to a massive increase in emissions, with humans activity contributing to 5.27 billion metric tons of CO₂ emissions just in 2018 alone [1]. The economic and public health impacts of global warming are continuing to harm society with the constant addition of emissions into our atmosphere and continual projected rise in average atmosphere and ocean temperatures [2] [3].

Mitigating the rise of these greenhouse gases will require significant changes to many aspects of the economy, including personal transportation. The automotive sector has historically been one of the biggest contributors to harmful emissions and is one of society's largest opportunities to reduce our emissions with changes in transportation technology [4]. The transportation industry was responsible for 28% of the global CO₂ emissions in 2018 [5].

New vehicle architectures, such as battery electric vehicles (BEV) and hybrid electric vehicles (HEV), have an opportunity to improve transportation efficiency, and thereby curb these emissions [6]. The possibility to provide power to the vehicle via traditional internal combustion engines (ICE) and with an electric motor (EM) opens many opportunities for gains in fuel economy. Changing the powertrain components in a vehicle is not the only area of opportunity for efficiency gains. The controls techniques used to address the vehicles energy demand is another opportunity for optimization, as the powertrain has another degree of freedom during operation if it utilizes a hybrid powertrain. The ICE and EM both have different characteristics of where they perform best, and novel approaches on how to best utilize these strengths can allow for further improvements to modern vehicles. Developing these systems present numerous

challenges due to the complex nature of integration a hybrid system, especially to non-OEM researchers.

The Colorado State University Vehicle Innovation Team has spent 2018-2021 designing, modeling, fabricating, and testing two separate hybrid vehicle platforms, with the goal of advancing new vehicle technology. The first vehicle was a stock 2019 Chevrolet Blazer that was transformed into a hybrid electric vehicle as a part of an intercollegiate competition sponsored by the U.S. Department of Energy's (DOE).

The second vehicle that CSU VIT has developed is a hybrid electric Toyota Tacoma truck. This project was a collaboration with Toyota Gasoline Hybrids R&D, with the goal of quantifying fuel economy gains with advanced controls techniques. These controls techniques are focused on acceleration events, as these events occur often with little variability, and require larger amounts of energy, making it an ideal candidate for fuel economy gains [7]. Both vehicles will serve as a test platform for testing new and innovative hybrid vehicle technology, as the intimate knowledge of the over all system the team will gain during integration gives a unique advantage for further vehicle development that would not be possible in a stock vehicle.

The purpose of this thesis is to provide an in-depth record and background on the development of these two vehicles, as well as lay the foundation for future students and researchers to learn from the experiences and results of these vehicle development projects. Both vehicles will have the capability to be test beds for several innovations, and thus a deeper understanding of both systems is necessary while further developing the system.

1.1 Background

1.1.1 EcoCAR Mobility Challenge

The EcoCAR Mobility Challenge is a four year long intercollegiate competition in which multiple teams in North America compete. This competition was a continuation of the EcoCAR series which is part of the U.S. Department of Energy's Advanced Vehicle Technology Competitions (AVTCs). This program aims to foster a learning environment for undergraduate and graduate students that is focused on new vehicle technology and to drive innovation and research in the transportation sector. The DOE challenges students with many tasks within this competition that are aimed at preparing students for careers in the automotive industry. Among these tasks includes an in-depth analysis and design of the hybrid electric system architecture.

The basis of the EcoCAR Mobility Challenge was to design and build a hybrid Chevrolet Blazer that appeals to a nascent mobility as a service market. This hypothetical fleet owned car-sharing service was the basis for many of the design decisions made throughout the project, as the teams target customer would want to take this vehicle into mountain ranges and would require at least 300 miles of range. This vehicle would also be judged on several other criteria such as: vehicle mass, braking distance, emissions, fuel economy, and consumer appeal. Another large aspect of the project was the integration of an SAE level 2 autonomous system within the vehicle. Many photos of CAD and the physical implementation have been omitted from this document as they contain confidential information.

1.1.2 Toyota Tacoma Test Vehicle Platform

The Toyota Tacoma Test Vehicle Platform (TVP) was used to demonstrate real world fuel economy (FE) gains by implementing a powertrain control strategy that utilizes predictive acceleration events (PAE). PAE based control schemes have demonstrated fuel economy gains in hybrid vehicles but integrating these complex control systems into stock hybrid vehicles is next to impossible without the help of the vehicle OEMs, as this process requires tools and knowledge that are not in the public domain. Thus, the CSU VIT was tasked with the challenge of electrifying a stock 2018 Toyota Tacoma by adding hybrid powertrain components, as well as a hybrid control system. This project was mainly completed by graduate students and did not have access to the extensive labor pool available within the EcoCAR project. The project started off with a stock 2018 Toyota Tacoma, that then had several hybrid systems installed into the vehicle. The PAE based control strategy requires full control of the ICE and EM, and thus the team had to implement a control system to actively test the PAE strategy against other baseline controls strategies.

1.2 Parameters that Effect Fuel Economy

There are many factors that come into play when considering and controlling for vehicle fuel economy. Physical vehicle parameters such as mass, aerodynamics, and even tire pressure all effect the vehicle's fuel economy regardless of powertrain configuration and vehicle type [8]. The driving style of the vehicle operator can also affect fuel economy, due to the influence gear

selection and acceleration rates have on fuel economy. Design choices in the vehicles powertrain can also influence fuel economy, as hybrid electric drive systems come with their own inefficiencies in the high voltage system, but can be utilized to achieve gains in fuel economy when compared to ICE powered vehicles [9] [10]. The focus of much research in recent years has been aimed at increasing fuel economy with hybrid powertrain control strategies, which seek to enable the optimal operating conditions for operation of the hybrid powertrain [11] [12] [13] [14]. Another budding area of research is focused on using connected and autonomous vehicle (CAV) technology to allow the vehicle to gather more information about its surroundings for better planning [15], where coordinated planning optimization, and operation can lead to improvements in vehicle efficiency and performance.

1.3 Predictive Acceleration Events

PAE are a way of optimizing energy use in hybrid vehicles by trading the vehicles energy demands to and from the electric drivetrain as a function of time. Acceleration events are interesting targets for this strategy as they have a high energy cost, predictability, and relatively limited variability [16]. Trading vehicle energy pathways in time allows for the internal combustion engine to operate within its most efficient region, regardless of the physical needs of the vehicles propulsion system. Any excess energy available to the vehicle is regenerated via the electric motor, as the energy required for vehicle propulsion can often be less than that of the power provided by the engine at its peak operating efficiency. The efficiency at which the electric motor can recoup this excess power happens to be higher when the power levels are lower. This means that the more power the vehicle requires for acceleration the less power is

available for recovery, thus leading to greater efficiencies in energy regeneration from the electric motor. Previous modeling work based on a 2010 Toyota Prius has illustrated the benefits of such pre-computed acceleration events [16] [17]. This modeling work outline the gains that PAE can have when compared to a baseline controls strategy, especially over a full drive cycle. Several drive cycles were identified to be the largest opportunities for FE gains. The main goal of building the TVP is to have a platform that is capable of repeatedly testing FE over AEs as well as full drives cycles, while easily being able to switch between a PAE and baseline controls scheme. This project will also allow the team to achieve a higher fidelity model of the system, and further refine PAE and prove FE gains with a real car rather than just a model.

1.4 Novel Contributions

The novelty of this thesis is found in the comparisons of the design considerations for two hybrid vehicle projects with different purposes, end goals, and overall project infrastructures. In much of the literature on hybrid electric vehicle detailed design, only one vehicle type, vehicle use case, and testing protocol is considered in the design process. By comparing and contrasting the design process for these two vehicles, this thesis seeks to build an understanding of how differing requirements for hybrid electric trucks/SUVs can be expressed through differing hybrid design strategies. This paper will aim to capture the design considerations for each project along the design, fabrication, and integration phases of the project.

This effort is also novel in that this project involves the first documented development of these types of predictive optimal energy management control-enabled hybrid vehicles. This type of vehicle is one that has the potential to become mass-market technologies, as the benefits of

PAE and other similar predictive energy management control strategies can be proven. These vehicles represent the first known prototypes of predictive controllable hybrid vehicles in the literature, and the documentation of their design and implementation will serve to inform future development of this technology.

Chapter 2: Design Criteria Comparisons

There are many differences in the design requirements of these two vehicles due to the differing nature of the end goal of the vehicles. The Blazer is geared more toward an end-product that customers may find in a showroom or rental fleet, whereas the Tacoma TVP is designed strictly for research purposes, and as such will have different fits, finishes, and features. The TVP also does not have an extensive set of guiding and restricting rules that must be followed, unlike the Blazer which was developed under the guidance of the EcoCAR Mobility Challenge. The EcoCAR rules helped in guiding the overall direction for the teams to maximize consumer appeal for the target market, while also pushing the boundaries of new vehicle technology. The EcoCAR rules are focused mainly on safety and the competition point awarding and deduction system that guides the deliverables, overall scope, and implementation of the vehicle. The safety and design standards put forth in the rules are however industry standards and thus many of these best practices were carried over to the TVP such as the FEA (finite element analysis) evaluation conditions of 8 Gs in the lateral and front to back direction and 20 Gs in the vertical direction.

On the other hand, the TVP is designed to meet a few set research goals and is purely functional, which loosens many constraints. This means that the team is not forbidden from taking up all the cargo area with instrumentation and components, unlike for the Blazer which the team gets penalized for infringing on the stock vehicles passenger and cargo capacity. It also allows the team to accept any quirks of the vehicle that would not be acceptable in a consumer vehicle, such as having to control the contactors via switches in the center console or having coolant lines run through the cab. This design freedom means that the team could make changes

to the vehicle if necessary, such as remove the air conditioning system, which is strictly forbidden in the EcoCAR program.

The level of industry involvement is also drastically different, as the sponsors for the EcoCAR project were more involved and willing to share confidential information, whereas the TVP could be completed without this level of intimate knowledge. The necessary communications database files (.dbc) and CAD files for the Blazer were given to all the teams in the competition, whereas this was not the case for the TVP. The level of information available changes much of the design and implementation work required to make the vehicle function and can add significant challenges and delays to the project. Not having CAD of the vehicle makes the component selection process more complicated, as you are often relying on physical vehicle measurements that can often be difficult or impossible to obtain. For example, selecting an electric motor that would fit on the tail stock of the transmission is difficult due to the complex geometry of the transmission tunnel along with the propeller shaft getting in the way of the measuring tool.

The serviceability of each vehicle also must be taken into consideration. The Blazer is a competition car, and as such is on very tight deadlines when it comes to the vehicle's performance. With this in mind, the design must consider the process in which a serviceable part can be replaced during the short maintenance time provided in the competition. The TVP has no such constraints, and thus can implement systems that may require a lot more time to service but require significantly less time to fabricate.

2.1 Autonomie Modeling

Autonomie is a tool that was developed by Argonne National Laboratory for the purpose of modeling powertrain configurations, control schemes, and new component technologies to quantify gains in fuel economy without having to physically build a vehicle [18]. Autonomie has been generally accepted as the industry standard modeling tool due to its strong correlation to real world testing data [19]. As described in previous work, it was determined that the model for the 2010 Toyota Prius is within 2% of real-world vehicle data [17].

CSU VIT has developed and simulated an Autonomie model of the TVP that included over 2,700 acceleration events and multiple controls schemes. This model was then used to determine if a pre transmission (P2) or post transmission (P3) hybrid would produce an increase in fuel economy. The table below shows the results of this study, which show that both a P2 and P3 setup are viable for the research goals, but the P2 slightly outperforms the P3 model.

Table 1. Average results of 2700+ AEs comparing pre and post-transmission models

	Baseline FE (mpg)	Optimal FE (mpg)	Delta FE (mpg)	% FE Increase	Baseline FC (mL)	Optimal FC (mL)	Delta FC (mL)	% FC Increase
P3	6.43	7.62	1.19	21.5%	35.45	30.17	-5.28	16.7%
P2	6.62	8.17	1.54	22.9%	34.71	28.88	-5.83	16.3%

2.2 Vehicle Architectures

In order to compare and contrast the design and integration differences between the two projects we first must take a step back and understand both vehicles' architectures. Overall selection of these architectures was done in conjunction with the component selection process, though there were many factors that affect these decisions.

There are many distinct ways to integrate an electric motor into a tradition ICE vehicle, which are describe using a P0-P4 nomenclature. A P0 vehicle typically utilizes an electric machine on the front of the engine and is usually belt driven along with other vehicle accessories. P1 architecture differ in that the electric machine is on the other side of the engine, and is coupled to the crank shaft and is installed between the clutch and the ICE. A P2 is the same as a P1, with the only difference being that it is installed between the clutch and transmission. P3 architectures have the electric machine installed on the end of the transmission at the output shaft. Lastly, a P4 is unique in that it is in the rear axle of the vehicle, and often is disconnected from the rest of the powertrain components.

The TVP was designed as a post-transmission (P3-parallel) hybrid where the EM is placed post-transmission and pre-rear differential. The Autonomie model predicted that this P3 hybrid setup would essentially perform the same as a P2 setup when comparing fuel economy. This consideration along with the simplicity of integrating a P3 versus a P2 were the main factors for selecting a post-transmission architecture. This would also allow the team to avoid having to separate the stock transmission and engine, which simplifies and already complex process of modifying the powertrain. The simplest way to integrate an electric motor in this configuration is to utilize and axial flux motor with a female through spline shaft to integrate directly onto the existing transmission output shaft. This architecture avoids the use of complex clutch systems and housing. This also would extend the transmission much further back in the vehicle, which

would create a large cantilever force on the entire powertrain. To this end, the electric motor was mounted onto the “tailstock” of the transmission, a conical aluminum cast part that covers the transmission output shaft until it reaches the output shaft slip yoke. In a four-wheel drive vehicle, the transfer case would be integrated in the place of the tailstock/EM setup chosen here.

The TVP retains the stock 2.7 liter 159 hp, 180 lb-ft 4-cylinder engine and six speed automatic transmission, as the scope of the project does not require a full powertrain redesign. This aspect also greatly reduces the design, fabrication, and installation work, thus allowing the team to reach the research goals sooner with less complications. Figure 1 below shows the Tacoma hybrid drivetrain layout.

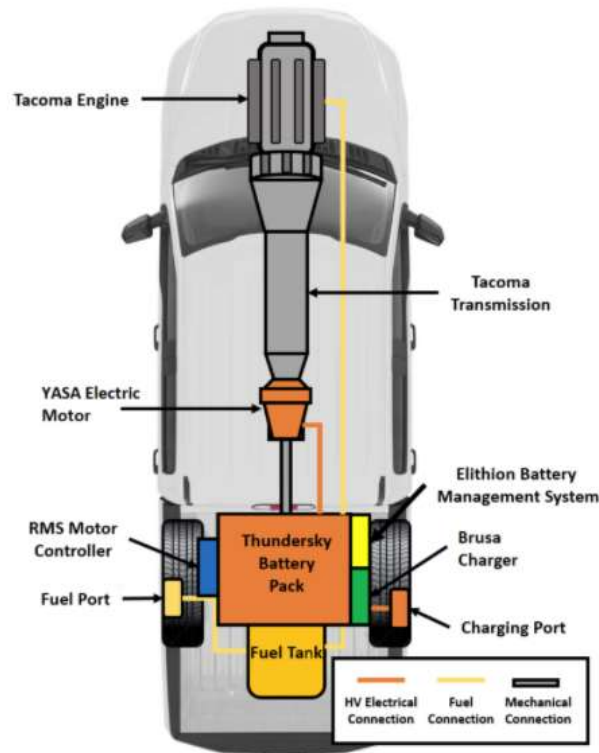
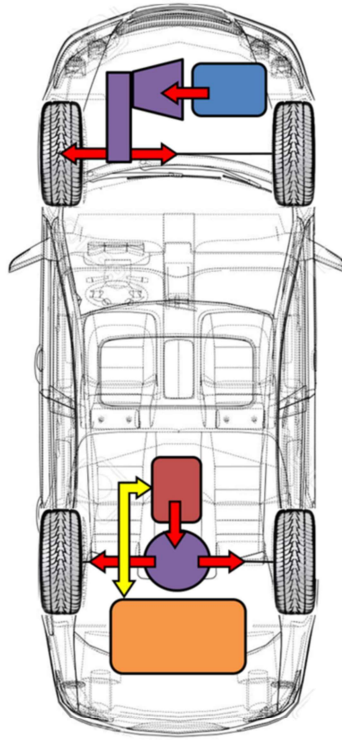


Figure 1: TVP architecture diagram

The 2019 Chevrolet Blazer was designed and built as a P4 parallel hybrid, in which the front and rear wheels are powered from separate power plants and are not connected. This architecture has many benefits. The main is ease of integration, as this configuration allowed the team to reach a functioning vehicle in a shorter amount of time. This is important as a large percentage of points in the competition are based on functionality of the CAVs system, which requires extensive on road testing. The team also wanted to avoid the integration challenges that the previous EcoCAR teams faced, with complex design and tolerances required to pull off a P1 or P2 powertrain configuration [20]. The stock 6-cylinder engine was replaced with a 2.0L turbocharged LTG engine from General Motors. This engine retained its stock 9 speed automatic transmission, but the prop shaft that connects the transmission and the rear differential was removed.

The rear differential (also commonly referred to as a rear drive module or RDM) that was mounted in the rear subframe was replaced with a Magna electrified rear axle drive system (eRAD), capable of providing 60 kW of peak power and 120 Nm of peak torque. Figure 2 below shows the Blazer hybrid drivetrain layout.



Legend
 Electrical Energy Flow ← yellow arrow
 Mechanical Energy Flow ← red arrow
 Mechanical Connections — black line

Figure 2: Blazer architecture diagram

Chapter 3: Component Selection

3.1 Electric Motor

The EcoCAR Blazer has a Magna eRAD installed in the rear subframe of the vehicle in place of the stock rear drive module. This design removed the prop shaft connecting the transmission and differential, which makes the vehicle a P4 configuration. This eRAD unit is capable of providing 90 Nm of continuous torque and 50 kW of continuous power, which allows the vehicle the torque capability to climb steep mountain grades, as this was one of the design requirements for the selected target market. The eRAD was also heavily discounted for this project, which helped sway the decision of the team, as this would free up resources for other high-cost aspects of the project. The ease of integration of this unit was also a factor as the team knew a more complicated architecture would result in a prolonged integration period. To install the unit this design required the removal of several stock components (power transfer unit, propeller shaft, RDM) and make a mount along with new half shafts. Due to the nature of the suspension and half shaft integration, this allows for larger tolerances when manufacturing and installing the rear subframe mount for the eRAD. This aspect of the design allowed for a quick install/uninstall of the unit as high precision tools and instruments would not be necessary for the installation of the unit, which was unlike past projects that utilized different powertrain architectures.

The component selection process for the TVP began with the electric motor power and speed requirements for the system, as packaging and integration for the remaining components is relatively straightforward in comparison to the electric motor. This is because the remainder of components can be located anywhere on the vehicle, as the car does not need to retain any cargo

space and the bed of the truck is a simple location to integrate components into. The motor selection process for the TVP was also largely driven by packaging constraints. To simplify the hybrid integration process, a post-transmission through-shaft motor would need to be selected, as this would allow for simple integration of the unit on the end of the stock transmission casting. This motor would also have to be around 12” in diameter or less to fit in the transmission tunnel, though if it were slightly over minor modifications could be made to the transmission tunnel.

The peak torque that was predicted by PAE simulations for the TVP was 350-400 Nm at 1600 RPM. The design process led to the selection of the YASA P400, as it is able to achieve the required power and speed requirements and also possesses a through shaft for in-line motor mounting. The unit was slightly over the ideal diameter to fit in the transmission tunnel. This was accommodated by slightly modifying the transmission tunnel, which was significantly simpler than creating custom designed powertrain components to allow the motor to integrate into the stock vehicle’s powertrain.

3.2 Inverter/ Electric Motor Controller

With the use of the Magna eRAD, the EcoCAR team was heavily incentivized to use the Magna ECO20 inverter, as this unit is tailor made for use with the eRAD. Selecting another inverter would add a significant amount of development time and effort, as many off the shelf units are not directly compatible with this eRAD. These other choices would have led to a new set of development challenges as the eRAD unit was treated as somewhat of a black box, and reverse engineering this black box was a more complicated effort than was desired. This electric motor controller (EMC) is also capable of handling more power than the battery can output, with

a maximum traction motor control current of 370 amps at 450 volts. The ECO20 Inverter unit is also 97% efficient, which is important as the battery capacity is not very large, and every gain in efficiency means more range from the vehicle. The inverter is also IP69 rated and is designed to be mounted in a large cutout in the underside of the unibody. This eases integration and packaging and allows the unit to act as a pass through for electrical and fluid connections.

The TVP utilizes a Rinehart Motion Systems (RMS) PM150DX motor controller and inverter. This unit was selected as it can handle the voltage and power that the YASA P400 requires, which is the main selection criteria. CSU VIT has experience with successfully integrating RMS inverters in multiple vehicles for past projects and is familiar with the calibration procedure. This unit is also compact enough to fit in the bed of the truck along with the other high voltage components. CAN compatibility is another feature that was a requirement for the EMC as it is critical for controlling, monitoring, and data collection.

3.3 Energy Storage System

The Blazer utilizes a battery pack manufactured by General Motors that is used in the hybrid Malibu, referred to as the HEV 4. This pack is a Li-ion NMC (Nickel Manganese Cobalt Oxide) battery consisting of 80 cells in series for a total energy capacity of 1.5 kWh and nominal voltage of 300 V. This pack is capable of discharging up to 52 kW, which is significantly less than the specifications of the Magna eRAD allow, and significantly less than the power required to drive the Blazer in a hypothetical EV mode.

This battery was a donated component from competition sponsors, which not only made it an attractive option from a budgetary standpoint, but also for the technical support that came

along with the pack. This option was also enticing because of the included functionality of the unit straight from the factory. This unit contained all the necessary high voltage components, all conveniently packaged in one unit that fits under the floorboard of the trunk of the vehicle. This circuitry includes the high voltage contactors, precharge resistors and relays, manual service disconnects (MSD), auxiliary power modules (APM), cell sensing boards, and battery management system (BMS). The APM, which converts high voltage DC to low voltage DC (12 volts), also allows the team to utilize the high voltage energy storage system to help power the energy intensive computational units required for the CAVs features. Ultimately the compact design and simplicity of the unit was the major driving factors for the selection of the unit, as this goes with the main design criteria, which is to get the car driving as quickly as possible. It also allowed the vehicle to retain almost all the cargo carrying capacity compared to a stock vehicle.

The Toyota Tacoma was integrated with a larger 13.46 kWh battery pack, consisting of 102 ThunderSky Winston LiFeYPO₄ cells in series, each with a capacity of 40Ah. This pack can deliver 400 A for 5 seconds, or 120 A continuously. These cells were selected over other cells on the market for several reasons. The main reason is that the prismatic cells are easy to install and mount into a pack compared to cylindrical or pouch style cells. These specific cells come pre-installed with threaded leads, which prevents the need for spot welding cells together (which is common in mass produced BEVs and HEVs). Battery spot welding makes the fabrication process more complex and riskier as well as lowers the reliability and serviceability of the pack. Servicing a spot-welded cell is also very dangerous, which is why BEV and HEV manufacturers do not want customers servicing the high voltage battery. The selected cell for the TVP also possesses high specific capacity and power, and the high current output capability means that the

pack can be a purely series pack without the need for parallel cells. Avoiding parallel cells cuts down on pack cost, complexity, and build time. A single 40 Ah cell is shown in figure 3 below.



Figure 3: ThunderSky Winston LiFeYPO4 40 Ah battery

The individual cells are monitored by an Elithion BMS. This BMS was selected for a variety of reasons, the main reasons being CAN communication capability, and simplicity of cell board wiring. Figure 4 below shows an Elithion cell board (uninstalled) which not only monitors temperature, cell resistance, and cell voltage, but are responsible for cell balancing during charging. Other BMS systems on the market require wiring each cell to the main unit, which is a lot of work from an integration standpoint when you have 102 cells. In contrast the Elithion system communicates to each individual bank rather than each cell, significantly cutting down on the work required to wire the monitoring system.

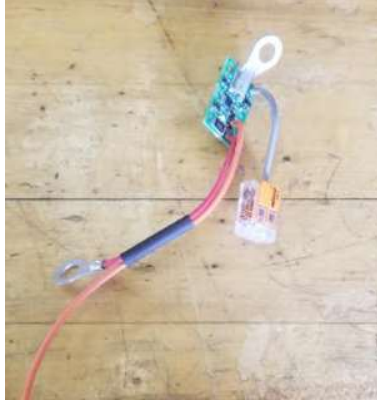


Figure 4: Elithion cell balancing board

The downside to building this custom battery pack compared to buying a unit similar to the HEV 4, is that to construct the TVP we had to build in the high voltage circuitry required for control. This also requires design and fabrication of housings for all these cells and components. This not only adds the task of designing and packaging these components, but also properly selecting them such that they are rated for the power the pack can deliver.

Adding a DC to DC converter to provide 12V power would add unnecessary complication to the Tacoma, as the design requirements of this vehicle does not require a robust EV mode that would meet consumer expectations. This does not restrict the team from simply adding a large 12V lead acid battery to the rear seat or truck bed of the vehicle if deemed necessary, and the 12V alternator from the ICE is present and operational in the TVP. The Blazer also has a higher auxiliary load, as the onboard processors require relatively large amounts of energy to run the driver assistance software. The TVP also has the luxury of being able to have special operating requirements that would not be feasible in a production level vehicle. For example, if the group notices that the vehicle is drawing too much auxiliary power such that there is an issue powering components, the team can simply shut off any stock vehicle loads, such as the air conditioner, radio, lights, and other auxiliary loads. This is in contrast to the design requirements for the

Blazer, which do not allow the user to turn off these amenities to use the driver assistance features.

3.4 Internal Combustion Engine and Transmission

The internal combustion engine selection was severely limited in the EcoCAR project due to the rules of the competition. GM was willing to give each team a selection of a few engines and would not support any other engines. The team ultimately selected the GM LTG 2.0L turbocharged engine, which is capable of producing 255 Nm at 4400 RPM. This engine is advantageous due to the fact that it comes with a forced induction turbocharger, which is important for the high altitude driving that the selected target market would be venturing into often. This engine does require the use of an air-to-air intercooler due to the rise in temperature of the intake air on the engine from the compression of the turbo charger. This engine also shares mounts with several other units that are factory options in the Blazer, making the integration of the engine relatively straight forward compared to other power plants.

The TVP utilizes the stock 2.7 liter 4-cylinder engine and six speed automatic transmission for several reasons. The main reason for not swapping the internal combustion engine is due to the added scope and complexity that an engine swap would add to the project. This is also unnecessary as the stock unit is capable of meeting the research goals presented for the project.

3.5 AC-DC Charger

High voltage AC to DC chargers (also referred to as on-board charger or OBC) allow a vehicle to charge its high voltage battery via an AC wall charger. The need for an AC-DC high voltage battery charger was not needed in the Blazer, as the vehicle was designed to be a charge sustaining hybrid. This means the vehicle utilizes the eRAD to regenerate energy from the vehicle's deceleration back into the high voltage battery. The plug-in option was omitted due to the lack of charging infrastructure in the location that the identified customer base would be using the vehicle at, as well as the complexity this would add from a business logistics standpoint. The small size of the Blazer's battery is appropriate for this type of charge-sustaining vehicle operation strategy. This also greatly reduces design and integration complexity as the team was already low on space, as the high voltage and CAVs components already had a large space claim in the rear spare tire well of the vehicle. The major downside of this method is the dependency of testing the high voltage system, on the driving of the vehicle. In other words, the entire car must be operational before the vehicle battery charging and discharging behavior can be tested. This puts vehicle operation as an early step on the critical path for the project which complicates vehicle development and testing. The use of an external high voltage power supply was used initially to charge the battery to a state of charge (SOC) that would be acceptable for testing.

The TVP originally was designed to use a liquid cooled 6.6kW Current Ways charger, as this unit was on hand from a previous project. This charger would be capable of charging the

battery completely in around two hours and is rated for use in automotive environments.

However, upon integration and testing the unit suffered a premature internal failure. The Current Ways unit was then swapped out with another on hand charger, the air cooled Brusa NLG5. This charger was very similar in terms of integration and wiring and does not require liquid cooling, which reduces the level of complexity of integration. The only downside of the Brusa is its charging rate is about half that of the Current Ways charger. This is not an issue as charge time is an aspect that is not important to the overall research goals.

Chapter 4: Development and Integration

4.1 Energy Storage System Enclosure

The battery that was selected for the Blazer is a fully enclosed and complete unit that contains all the necessary high voltage components for operation. However, the risk of high voltage exposure is still present, as the high voltage battery leads must exit the battery pack and enter the inverter. Because of these safety considerations another level of safety and security had to be integrated in the vehicle to prevent exposure. The high voltage battery was mounted behind and below the rear seats of the vehicle, with a new floorboard to be fabricated and placed over the unit. This lowers the overall cargo capacity of the vehicle, which counts against the design criteria of the EcoCAR Challenge. This compromise was unavoidable, as packaging the unit was challenging due to its physical size which does not fit under the stock floorboard. The other alternate position for the battery pack was under the vehicle. However, this comes with its fair share of integration challenges, as an external shield must be fabricated to protect the pack from the harsh environmental operating conditions present under the vehicle. Figure 5 below shows the mounting location of the HEV 4 battery in the spare tire well in the rear of the vehicle.



Figure 5: HEV 4 installed in the rear spare tire well of the Blazer (APM not shown)

The inverter used in the Blazer was purpose built to mount in a large hole in the floor panel of the vehicle. The team utilized the packaging benefits of this mounting style, and thus cut out the proper template of the unit in the rear spare tire well of the vehicle. This allowed the team to utilize the inverter as a pass through to route cables as well as coolant hoses. The low profile of the inverter also allowed the team to package the hybrid supervisory controller (HSC) the team selected to control the hybrid powertrain of the vehicle as well the computational units (Intel AIoT Tank, and Invidia Jetson) that provide the control for the driver assistance features. The following figure illustrates these benefits, as it shows the underside of the vehicle with the inverter installed in the rear spare tire well of the vehicle behind the HEV 4 battery pack.



Figure 6: Inverter installed into the rear spare tire well of the Blazer as seen from the underside of the vehicle

For the TVP, the high voltage battery enclosure is located in the bed of the truck up against the rear of the cab, and serves as the housing to protect the high voltage components from the environment, from dropped objects, as well as from anyone seeking to touch any high voltage components. This enclosure (shown in Figure 7 below) contains the EMC, OBC, BMS, contactor box, high voltage junction box (HVJB), and a 17x6 array of battery cells, for a total of 102 cells in series that produces a nominal voltage of 326.4 V.

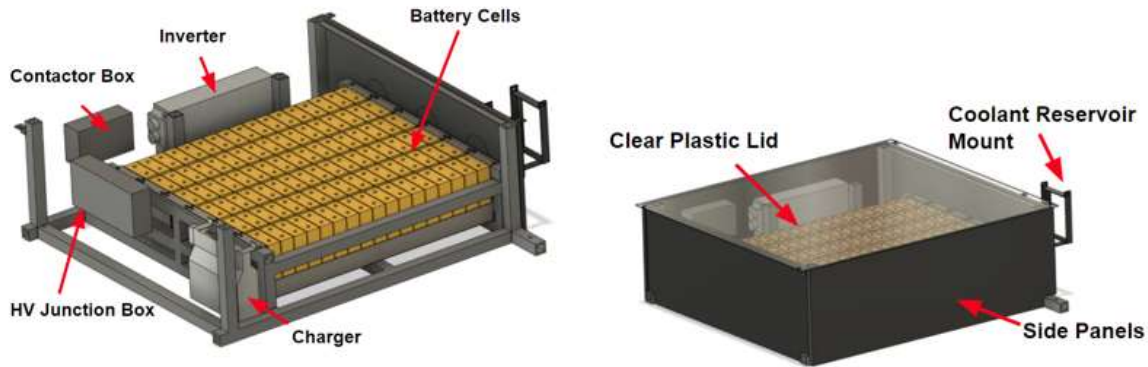


Figure 7: Battery box CAD renderings showing the components and frame, with and without the side panels and clear plastic lid

The array of battery cells are split into 6 banks, each containing 17 cells. Each of these banks get connected in series to form the overall pack. The connection in the two center most banks of the pack are not simply connected like the other banks, as there is a manual service disconnect that each side of the pack is connected to. The MSD allows the team to essentially breaking the continuity of the pack, rendering the positive and negative side of the battery discontinuous. This is important for safety during the integration and testing phase, as many tasks needed to be performed on the high voltage system after its fabrication, and proper use of the MSD is vital in completing these tasks safely. The manual service disconnect also houses the battery pack's fuse, which is a 350 A fuse. This fuse was selected based on the time it would take to open the circuit based on high power draw scenarios as well as a short circuit scenario. This particular fuse will blow less than a second if it sees a short but would not blow until about four minutes at the peak amperage the battery can discharge. This component is mounted on the side of the battery box, as seen below in Figure 8.



Figure 8: Manual Service Disconnect inserted into the receptacle on the TVP

Each of these battery banks described above are mounted in a tray that was fabricated from water jet cut sheet metal that was bent to shape. The batteries are restrained from motion in the front to back, and side to side orientation due to their contact with the battery trays. The vertical motion was restricted by two composite 90° angle stock with a layer of low durometer elastomer affixed to it. The elastomer is critical for closing the gap between the batteries and angle stock, as the fabrication method of the tray allowed for a slight sag in the center of the tray, which introduced the small gap. Figure 9 below shows a tray after manufacturing and before any components were installed.



Figure 9: Battery tray before installation

The internal frame of the box was welded together using square steel tubing, to which the batteries, inverter, and charger are all mounted to. This square tubing was selected due to its strength, and simulations demonstrate that under the loads of an accident the frame will retain all the high voltage components mounted to it at under its yield strength. The square tubing was also the mounting point for the side panels of the battery box, which were made from durable, fire retardant melamine boards. This side panels were used as mounting points for several components, such as the contactor box, high voltage junction box, J1772 charging circuit housing as well as many low voltage electrical connectors and cable management solutions. The lid of this box is comprised of a clear acrylic panel with aluminum angle stock surrounding the panels for structural rigidity and to act as mounting points for the hinges and locks. A water-resistant truck bed cover was also installed on the vehicle to protect the battery box should it rain during testing. Figure 10 below is an image of the battery frame and modules, while figure 11 is the completed box with all the components installed in the rear of the bed.

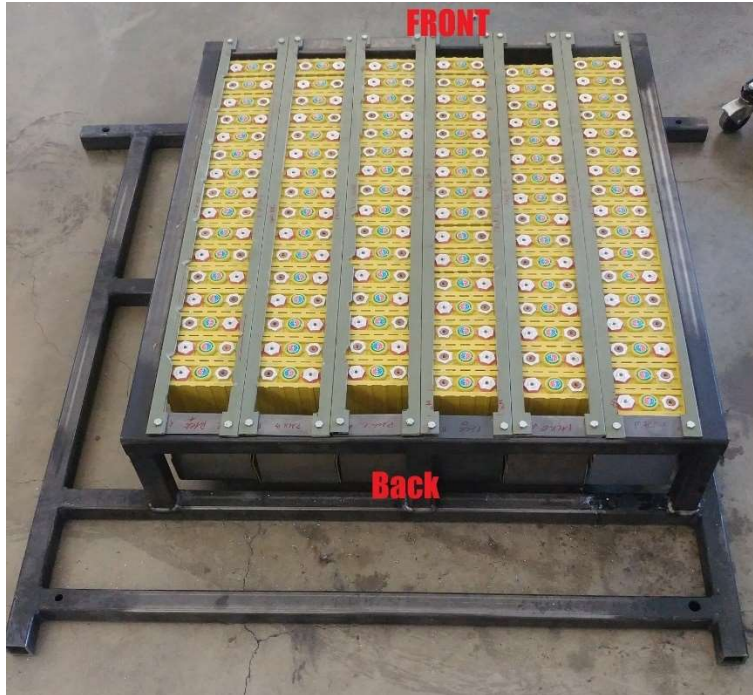


Figure 10: Welded battery enclosure frame with all 102 battery modules installed



Figure 11: Battery box installed in the bed of the Tacoma with the protective plastic lid shut

4.2 Battery Management System

The battery management system of the Blazer is internal to the selected HEV 4 battery pack. This significantly reduced the amount of planning and integration work the team needed to complete, as the BMS was functioning upon receipt, and was communicating via CAN all the important battery parameters the team would need to monitor. Many of the intimate technical details of the BMS were not provided to the teams, so this unit was treated as a black box that could not be modified. This was actually a benefit to the design, as the team did not have to spend time figuring out the correct setup for the BMS that would coincide with the battery pack and arrangement, as well as the integration of other high voltage components, such as the contactors.

For the TVP an Elithion Pro BMS was installed in the high voltage battery enclosure, right above the six battery banks. The BMS was wired in the hybrid power and CAN control system that was added by CSU VIT. This unit is also responsible for closing the high voltage contactors and precharge circuit, as well as monitoring the current coming in and out of the high voltage battery. The BMS's low voltage system can be powered by pin 2-Load Power (electric motor) or pin 3-Source Power (charger) depending on if the load or source is responsible for the SOC change of the battery. This is done by wiring pin 2 to the stock vehicles run mode power lines, and pin 3 to the auxiliary output of the OBC. However, through testing the team verified the BMS's function does not change depending on the pin that provides power to the unit. The current sensor and CAN current messages from the OBC and inverter are the method in which the BMS determines if the load or source is on. Either way, the main function of the BMS is to

shut off the pack if a cell potential diverges out from the specified voltage or temperature range, and it balances the cells during charging.

The individual battery banks, contactors, and current sensor are all connected to the BMS via a four pin Molex connector. Each battery cell has one cell board bolted on to each of its battery leads, along with a Wago lever nut connector that connects a single wire to the board before and after it, forming a communication network within the bank. The highest potential positive and lowest potential negative cells in each bank have a different style cell board that has a two-pin female Molex connector mounted to the PCB (printed circuit board). Both ends of each bank are then put into one four pin Molex connector that connects a single bank to the BMS. This method of wiring and monitoring of cells is preferred to other products on the market that require wiring two separate leads for each battery directly to the BMS. This distributed system avoids tedious wiring and difficulties of managing 204 individual wires. This centralized system also does not report individual cell temperatures, which is critical during charging of Li-ion batteries.

A major drawback of the Elithion BMS and cell boards is the low amount of current they are capable of dissipating during balance charging. The cell boards use passive cell balancing, where the board is responsible for dissipating energy out of the battery, which is less efficient than active balancing which transfers energy of one cell to the next. Each cell board can only dissipate 0.2 A, which is not very much current when compared to the charging capabilities of the system. The battery pack can charge at 120 A while regening through the YASA or 16 A when utilizing the OBC. This effectively means if any of the cells in the pack reach the desired state of charge before the rest of the cells, the entire pack must charge at 0.2 A, or else the cells with a higher SOC will charge past their limit and become a safety hazard. This is not an issue

for packs that are well balanced, but for packs with a few cells that rise quickly in SOC, this can be an issue and cause severely prolonged charge times.

Another vital function the BMS provides is a method of determining and reporting the packs SOC. There are two methods of determining a batteries SOC, voltage translation and Coulomb counting. Voltage translation is effectively measuring the battery's voltage and relating that back to a known SOC vs voltage curve. This is effective for traditional lead acid batteries, as the battery potential varies significantly over the batteries range of SOC. For many Li-ion battery chemistries the voltage is relatively constant in the middle of its SOC curve, and only begins to have significant changes towards the ends of the curve. "Coulomb counting" on the other hand integrates the current that has been drawn from or put into the battery to model SOC. This method only tells you the relative charge to a known starting point, which is sufficient for the research questions that the TVP design is trying to answer. This SOC parameter is important in determining energy efficiency gains in the PAE control method.

The BMS has proven itself as the least robust and reliable component on the vehicle. This is due to a variety of quality issues. The main quirk of the unit is that communication with cell boards can often be lost during the initial activation of the inverter and BMS. The team has experienced instances in which connecting to the BMS's GUI (graphical user interface) can reset some of its programmed parameters, which can also cause the battery to fault out or lose communication. A list of all programmed parameters for the battery pack can be found in the appendix. The SOC that is calculated by the BMS is also not accurate. The reported SOC from the BMS will go from 98% to 5%, when the SOC has actually only dropped by 5%. The BMS can also unpredictably lose communication with individual cells, or even whole banks. This

often happens during the startup phase, but can also happen while driving. The remedy for this issue cannot be solved with software changes, and the unit must be manually power cycled.

4.3 High Voltage Wiring

The following figure is the high voltage wiring system for the Toyota Tacoma TVP vehicle. This figure shows the high voltage wiring that begins at the high voltage battery, and routes through the contactor box, then to the junction box where the high voltage rails are connected in parallel to the high voltage charger, inverter, and high voltage test connection leads.

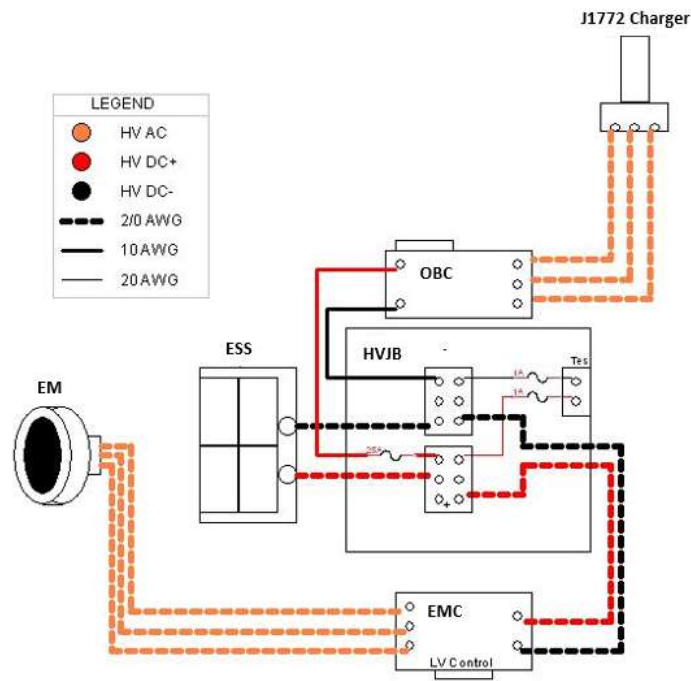


Figure 12: TVP high voltage wiring diagram

The Blazer's high voltage wiring diagram is similar to the TVP, with a few minor changes. This system achieves the same functionality, the main difference being that the battery module provided by GM has the contactors and precharge circuit internal to the pack. This battery unit also has an externally mounted APM which allowed the vehicle to power the low voltage system off of the high voltage battery, thereby enabling engine-off operation. The Blazer also does not have an OBC on the high voltage bus which further simplifies the design.

Figure 13 shows the physical routing of the high voltage wiring (shown in red) of the battery box on the TVP. This figure outlines the connections of each of the banks within the battery.

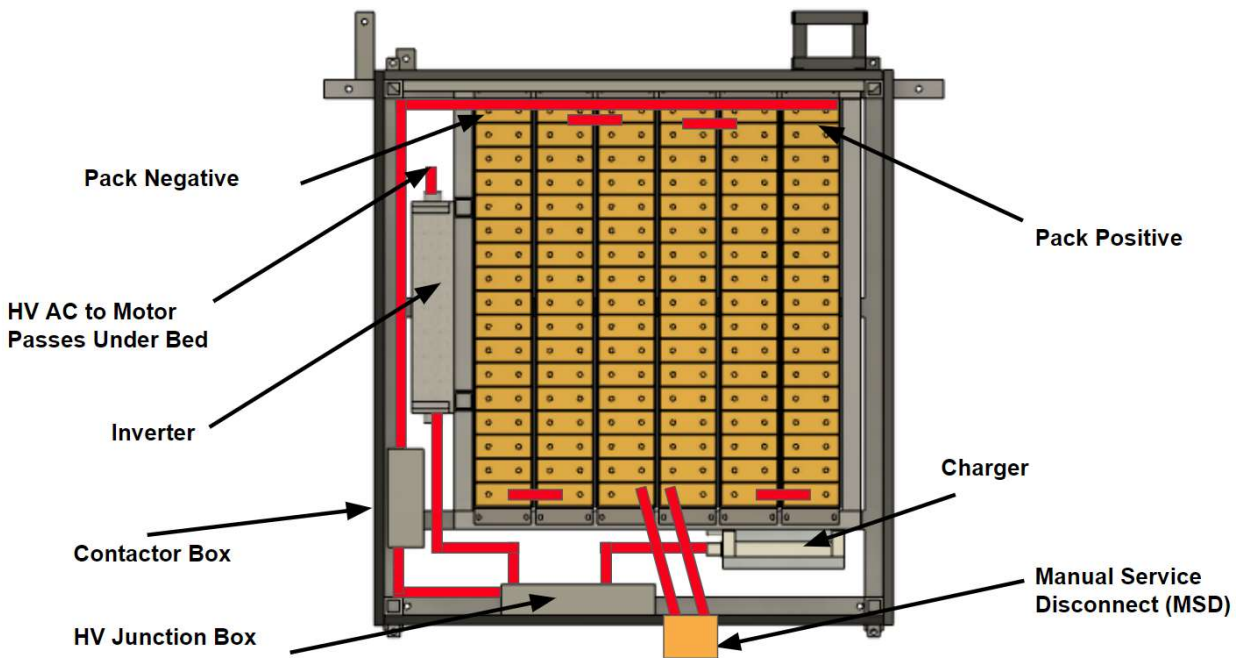


Figure 13: TVP high voltage battery routing diagram

Connecting the high voltage components is not a trivial task, as there are many considerations to keep in mind when designing and fabricating high voltage systems. Each of these projects utilized EXTRAD XLE 150 shielded high voltage cable from Champlain Cable, as it meets SAE J1654 for high voltage systems. This cable also contains a metal braided shielding layer outside of the main conductor and insulation, which reduces the effects of electromagnetic interference (EMI) when this shielding is properly grounded. These three inner layers are surrounded by a thin wall elastomer to provide chemical and thermal resistance to the operating environment of the cable. This type of cable is ideal not only for its electrical and thermal performance, but also for the tight minimum bend radii that are capable with these cables. Packaging these cables is often the hardest part of the design, as these cables are often routed in tight spaces and through body panels.

Physical connections were made in several different ways, depending on location. Many high voltage connections were simply made with copper ring terminals on stud style junction blocks, while other connections utilized heavy duty power connectors. The high voltage wires that are connected at the RMS EMC require wire ferrules, as they are retained by a screw style terminal block. Without the ferrules, the wire strands would be unconstrained and loosen over time due to vehicle vibration during operation. These ferrules also prevent the splayed wire from coming loose inside the inverter and causing a short circuit. Any high voltage wire that entered an IP (Ingress Protection) rated enclosure (such as EMC, contactor box, junction box) entered via a NEMA gland. Before the glands were tightened, the team ensured that the elastomer sleeve was properly seated against the cable gland fingers, as without this component the assembly will not have the proper ingress protection. A smaller sized washdown enclosure was utilized to connect each of the high voltage leads of the inverter and the EM together. One larger washdown

enclosure could not be used due to the tight packaging constraints of the frame rails in which the high voltage cables were routed. In this enclosure a screw style butt connector connected each section of the wire, which eases the disconnection and connection of these high voltage components during service. Figure 14 shows one of the three high voltage connection points.

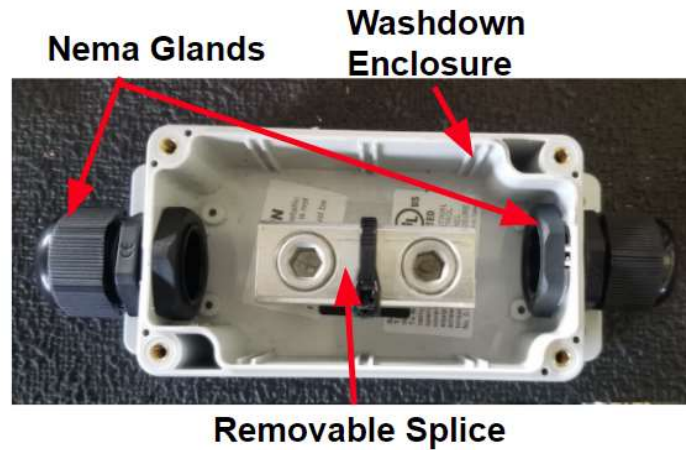


Figure 14: High voltage connection protected via a washdown enclosure for the TVP

Anti-abrasion tape was applied around the cable, and grommets were used for any location in which the cable passed through a body panel. This prevents premature failure or a short in the high voltage system cause by vibrational wear. The frame rails of the truck also allowed for an easy installation and routing of the electric motor and inverter connection, as the high voltage wire was placed in the vacant frame rail and was protected from the harsh underside environment of the vehicle, eliminating the need for split loom conduit to be applied. Depending on the specific location of the wire and its proximity to the exhaust routing, heat wrap tape was applied to the cable, and a heat shield was fabricated to further protect the high voltage wiring from the high exhaust temperatures. This was especially important in the Tacoma TVP, as the post

transmission YASA electric motor had high voltage connections that terminated into the motor within 2 inches of the exhaust.

This exhaust concern however was not an issue for the Blazer, as the high voltage components were all centrally located, and the routing of these cables was simple and did not pass near any high temperature components. In this vehicle however, the high voltage cables were forced to be routed between the vehicles rear subframe and unibody. To prevent any pinching of the high voltage cables a crush proof conduit was installed around the cable. This practice is recommended for any high voltage wiring that is routed under the vehicles and unprotected by another components, such as the frame rail in the Tacoma design.

4.3.1 Contactor Box and High Voltage Distribution box

The purpose of the contactor box is to act as the “on/off switch” of the battery, as the nature of the chemical energy storage of batteries does not allow you to “turn off” the battery. This can be problematic, as it is necessary to turn off low voltage power to the high voltage components, such as during an emergency situation when the EDS is pressed, or during component reboot which is often needed during integration and troubleshooting phases. Being able to control the high voltage system is very important not only for safety during operation, but also during the integration and testing phase.

The contactor box also houses the precharge circuit, which is vital for component health and reliability, as well as user safety, as this component soft starts the system. This soft start prevents a large current inrush on the input filter capacitors inside the charger, APM, and

inverter. Equation 1 below describes a simple capacitive circuit with a power source and no resistor.

$$I = C * \frac{dV}{dt} \quad \text{EQUATION 1}$$

This equation describes the capacitor element relationship between current and voltage, and how a large voltage can cause large inrush currents. The voltage supplied from the battery changes almost instantaneously as the contactor closes, which leads to a large inrush current when capacitance is high. A pre-charge circuit allows for this inrush current to be limited by a resistive element during contactor closing. The high voltage wiring of this pre-charge circuit can be seen below in Figure 15.

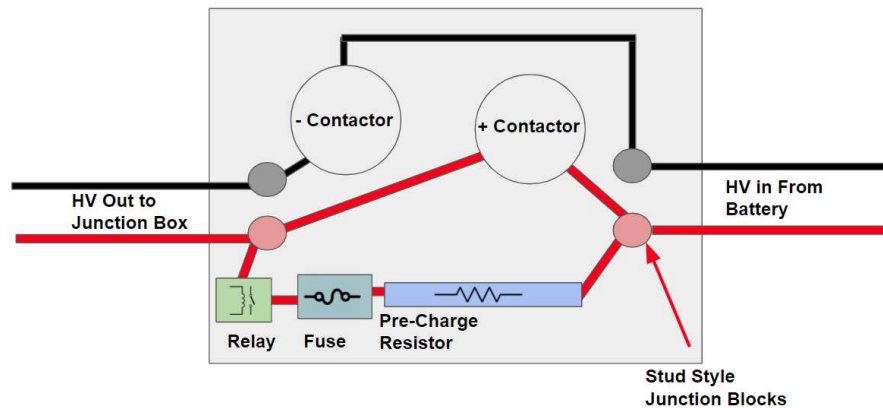


Figure 15: TVP contactor box wiring diagram

The contactors are the “on/off switch” for the battery, and have the potential to make or break the high voltage connection between the junction box and the battery. The negative lead of the battery contains this simple switch, whereas the positive lead is more complex as it contains the precharge circuit. The precharge circuit is in parallel with the positive battery lead and contactor and contains a resistor to control the charge time of the capacitors on the high voltage system. This precharge circuit can be activated and deactivated using a lower power relay rather than a larger contactor, as the currents the component will be subjected to are much smaller. The Elithion BMS uses the following nomenclature for the contactors and precharge relay in the BMS GUI as well as the CAN messages from the BMS:

K1: Precharge Relay

K2: Positive Contactor

K3: Negative Contactor

The process for soft starting the high voltage system is as follows:

1. Activate the negative lead (K3)
2. Activate the precharge relay (K1)
3. Wait for the capacitor voltage to charge up
 - a. Best practice is 5τ (time constant), as this is when the capacitor voltage will be at about 99% of battery voltage, thus reducing the change in voltage over time in equation 1 to a lower value. This however can be set to a reasonable time (a few seconds) if the proper precharge resistor is selected. A further explanation of this is given below.

4. Activate positive lead (K2)

- a. It is important to wait until the contactor is closed and debounced, as you need some small amount of overlap time with K1 and K2 both active or else the circuit could be broken. This is important to consider if there is custom software controlling this, as sending a signal to close the contactor, and the actual closing of the contactor do not happen simultaneously. For TE EVC series contactors this time is around 20 ms.

5. Deactivate precharge relay (K1)

The selection of the precharge resistor can be aided with the following calculations that allow for properly sizing the resistor and other pre-charge components. A MATLAB script of this resistor sizing guide and inrush characterization graphing is provided in the appendix. This script only requires inputs for the capacitance of the system, battery voltage, and desired pre-charge time. The script starts with the calculation of the proper resistance based on the capacitance, desired precharge time, and percentage charge on the capacitor (equations 2-5 below). The charge on the capacitor was set to 5τ , as this is when the capacitor is charged to 99.33%, which is considered best practice. With the calculated resistance, the simple RC circuit voltage and current can be solved as a function of time (equation 4 below)

$$t = 5 * \tau \quad \text{Equation 2}$$

$$R = \frac{\tau}{C} \quad \text{Equation 3}$$

$$V_c(t) = V_b(1 - e^{(-t/RC)}) \quad \text{Equation 4}$$

$$I_c(t) = \frac{V_b - V_c(t)}{R} \quad \text{Equation 5}$$

To properly select the resistor, you must also know the power that the resistor will be exposed to. This can be calculated by looking at the energy dissipated over time by the resistor, which is found by equations 6-7 below, which equates the power dissipation to the amount of energy stored in the fully charged capacitor.

$$E = \frac{C * V^2}{2} \quad \text{Equation 6}$$

$$P = \frac{E}{t} \quad \text{Equation 7}$$

This equation therefore calculates average power, and not peak power. This is often sufficient for the electrical design, but to get a better idea of the power dissipation you can graph the following equation, which finds the exact power dissipated as a function of time.

$$P(t) = I(t)^2 * R \quad \text{Equation 8}$$

The voltage and current of a simple capacitive circuit with a resistor can be analyzed using these equations. The MATLAB script given in the appendix models the prescribed resistor and power rating for the resistor, as well as the following graphs, which shows the voltage and amperage of the capacitors on the high voltage bus and the power dissipated by the resistor.

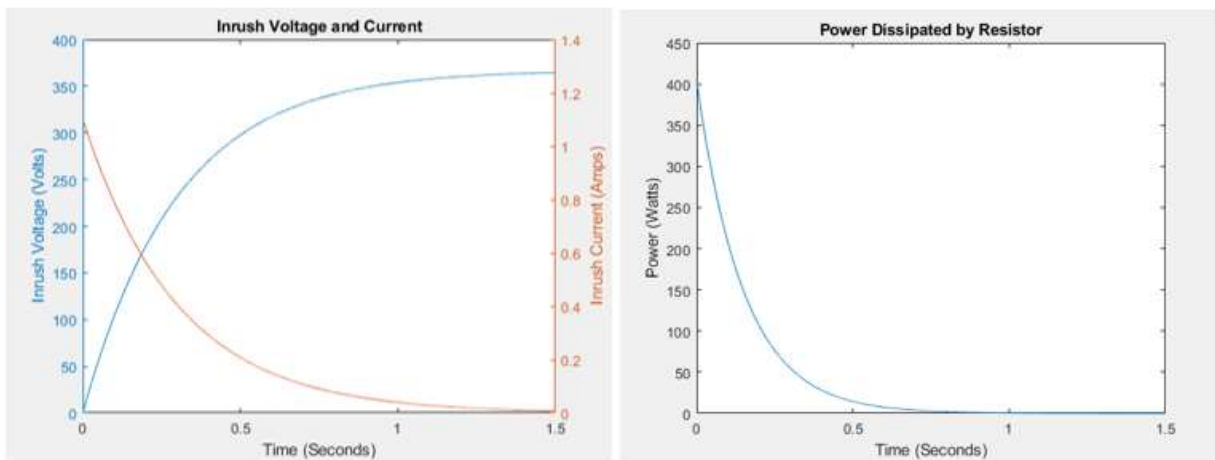


Figure 16: Pre-Charge resistor charging characteristics for TVP high voltage DC bus

As is visible in Figure 16, the largest inrush of current happens at the activation of contactors, as this is when the capacitors are charging up with maximum current. The script also gives the user the option to change the resistance of the circuit if modeling inrush current with different off-the-shelf resistors is desired, or with the low resistance of just the wires in the system. The resistance of the high voltage wiring from the battery lead to the inverter is around 0.15 ohms on the TVP, which results in a current spike of around 2447 A almost instantaneously, if no pre-charge circuit is in place. This tool may be useful to analyze if a pre-charge resistor is

needed to protect components for smaller, non-automotive battery systems. Looking at the graph of power will allow the user to better select a rated resistor for the system, as many resistors are rated for continuous power, but can momentarily handle more power than they are rated for. This graph of power can help identify if selecting a smaller resistor is appropriate, as it will show how much power is delivered over time.

In other examples of these types of design and simulation tools, Ozguc [21] has shown that a pre-charge circuit can achieve this same soft start effect but with a MOSFET activated by a PWM signal (Pulse Width Modulation) rather than a large pre-charge resistor and relay. This method could potentially save weight and cost while increasing reliability but requires a lot more development in the control software and hardware to achieve these gains. This may be advantageous for production level vehicles, but for prototype vehicles this adds too much complexity for the small realized benefit.

The high voltage distribution box contains two bus rails and serves as a point of connection for the battery, charger, inverter, and high voltage test connector. The high voltage wires enter the washdown enclosure via NEMA gland ends and are all terminated with copper ring terminals. The bus rails in which these copper ring terminals are affixed to are solid copper bars (approximately 1x2.5x10 cm) that are isolated from the box via electrically isolated standoffs. The figure below shows the physical implementation of these components.

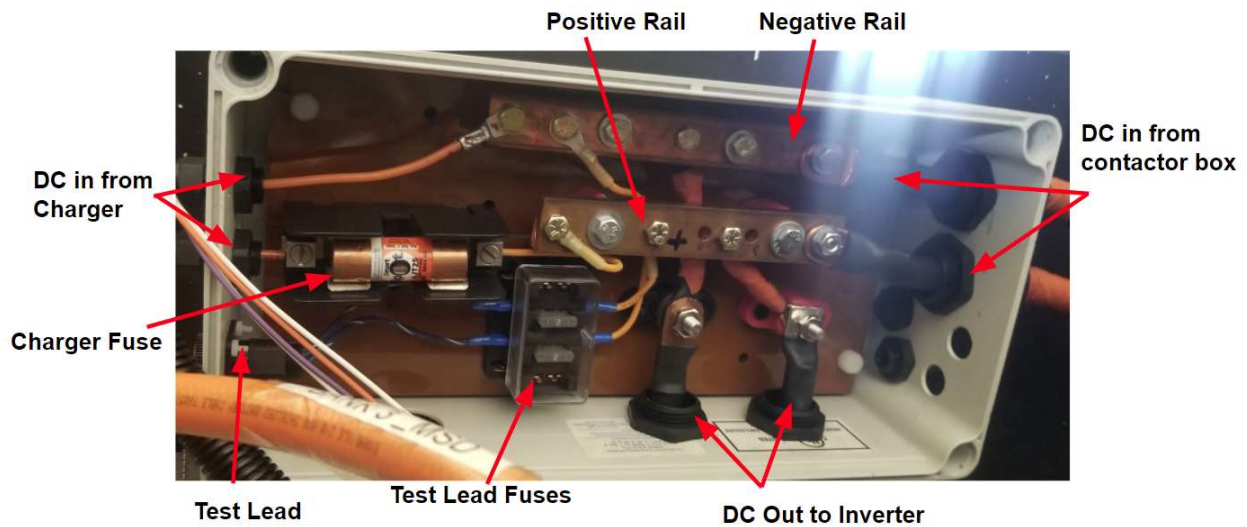


Figure 17: High voltage junction box

Both the contactor box and high voltage distribution box are isolated from the outside environment to prevent any unwanted exposure to high voltage. This is achieved by having a sheet of ¼ inch thick Garolite mounted to the washdown enclosure, and all the components within the box mounted to it. Garolite (G10 – FR4) is a composite material with high strength, excellent electrical insulation properties, low thermal expansion, low water absorption rates, and meets UL 94V-0 standards for flame retardance. This material is commonly used for PCBs and its material properties allow it to work well for this application. The material is not difficult to work with but does require good ventilation and proper PPE as it does create a high amount of dust.

4.4 High Voltage Charging

The charging protocol of modern Li-ion batteries call for two separate phases of charging, which complicates the charging process. For lower SOC's the battery must be charged using a constant current power supply, as battery voltage has significant increases going from lower to higher SOC's. At around 60% SOC, the battery must then be charged with a constant voltage power supply that decreases the current as SOC continues to rise [22] [23]. Due to the nature of the EcoCAR competition and lack of need for a high voltage charger on the Blazer, the team simply utilized a high voltage power supply to charge the battery when needed. This method is not as ideal as it must be constantly monitored to make sure proper charging techniques were maintained. This allowed the Blazer design to avoid packaging a charger in an already tight area of the vehicle, so the extra effort to design a charge sustaining system was justified.

The TVP does have an integrated OBC, which is a Brusa NLG5 that utilizes the SAE J1772 standard charging protocol and hardware [24]. The vehicle does not have a permanently installed charging receptacle, but rather has a low voltage and high voltage connector that connects a charging receptacle to the OBC. The charging receptacle can then be disconnected and stored outside of the vehicle while the charger is not in use. This design choice cuts down on the effort of having to integrate the receptacle into the vehicle's body panels. The cut out for the receptacle would not only need to be waterproof, but it also needs a custom cover to protect the charging port from debris, which would have added significant time and complexity to the high voltage system.

This charger has five separate high voltage wires, two of which connected to the vehicle's high voltage DC rails, and three come from the EVSE (electric vehicle supply equipment). The

charger connects into the vehicles low voltage power and communication system, as well as the low voltage J1772 communication protocol. The Brusa charger does not have the required internal resistance and switches that are necessary for the J1772 protocol [25], so an external washdown enclosure with the proper circuit was installed adjacent to the charger on the high voltage enclosure walls. This circuit was built and soldered onto a protoboard that was then waterproofed and potted using electronics grade silastic (silicone) to protect the delicate circuitry from the vibrations of the vehicle. The purpose of the circuit is to change the resistance measured on the proximity pin, which is one of the low voltage pins on the charge receptacle. However, the Brusa charger works in the opposite fashion as the J1772 protocol specifies, in that the resistance when the external circuit is in the off position is actually what makes the unit function rather than the proper on position. The following Figure shows the physical locations of these connection points on the EVSE that are not installed in the vehicle.

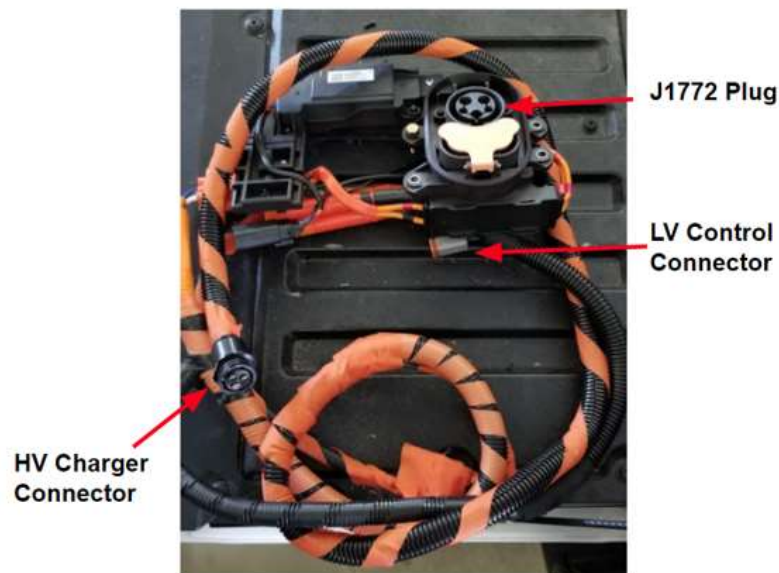


Figure 18: TVP EVSE plug with connection callouts

4.5 Low Voltage Wiring

The low voltage wiring work that CSU VIT was challenged with for each vehicle was drastically different. The Blazer was significantly more complex due to the nature and scope of the program. The root cause of the complexity was due to the internal combustion engine swap, which was difficult to integrate due to the incompatibility of signals and connectors for the engine, wiring harness, and body control module (ECM, TCM, BCM respectively). The Blazer also required a total of seven extra sensors for the self-driving system along with two computational units to process the data and communicate this with the HSC, which added a significant amount of wiring to the vehicle.

Each vehicle utilized a relay/ fuse box, which would control the power going to each of the added devices. These relays are controlled via the HSC, which allows the team to strategically activate or deactivate components at will. The physical routing of most of the low voltage system is routed into the cab of the vehicle and into the trunk/bed, connecting the front and rear components. All the wires are protected via a plastic split loom conduit, with the proper gromets installed for passing through body panels. Each wire is also labeled at each end with a heat shrink label, which is much cleaner and more robust than the typical method students use of wrapping electrical tape around a wire for a label.

4.5.1 Emergency Disconnect Switch

The emergency disconnect switch is arguably one of the most vital parts in the entire vehicle. The design and integration of the EDS is identical in both vehicles, as the function it serves is the same. The switch is a large red button that deactivates the vehicle when pressed and is intended for use during emergency situations to deactivate the hybrid powertrain. There are two emergency disconnect switches, one on the outside of the vehicle, on the rear bumper, and one on the dashboard of the vehicle within reach of the passenger and the driver. This switch is wired directly into the vehicle's relay/ fuse box and disconnected the power rail of the power relays for all the added components. This system does not shut off any stock vehicle systems, as it would be dangerous to shut off these components, such as the power steering system. Figure 19 below shows the location of the emergency disconnect switch on the rear bumper of the vehicle.



Figure 19: Emergency disconnect switch installed on the rear bumper

4.5.2 Wire Selection

Selecting the correct size wires for the vehicle is critical, as if this is done improperly it can lead to several issues. The resistance of a wire is inversely proportional to the cross-sectional area of the conductor. This means if a wire is too small it will have a larger resistance, which heats up the wire due to ohmic heating and can cause the insulation to degrade and cause a short circuit and in some cases a fire. In contrast, having a wire that is oversized can have several downsides as well, however they are all significantly less catastrophic. Using larger wire makes a car heavier, more expensive, and harder to design as the bend radii of wires decrease as wires get larger, making them harder to route through the vehicle. Due to these factors the team typically selected wires a gauge or two oversized to account for uncertainty in the system operation and design.

To select the correct size wire, the designer must know the electric current draw, voltage, and temperatures the wire will be exposed to. Unfortunately, one must often test the component in the vehicle or on a test stand to physically measure the current draw of a component. If a physical test is unable to be performed (due to timeline or budget constraints) then the continuous current rating of the components can be substituted for the test data. This data can then be used to simulate the steady state temperature of the wire given the ambient temperature the wire is exposed to. This heat transfer problem can be solved with Equations 9-11 below which equates the heat transfer loss rate per unit length to the heat generation rate per unit length [26]. Equations 10 and 11 model the ohmic heating and Fourier's heat conduction equation for heat generation and heat conduction respectively, where I_{rms} is the current through the wire, R is resistance and R_{th} is thermal resistance.

$$q_{Gen}^I = q_{Loss}^I \quad \text{Equation 9}$$

$$q_{Gen}^I = I^2 * R \quad \text{Equation 10}$$

$$q_{Loss}^I = \frac{T_{Wire} - T_{Ambient}}{R_{th}} \quad \text{Equation 11}$$

The thermal resistance of equation 11 takes into account the conduction via the insulation, convection to the surrounding environment, and radiation. To simplify the model, an R_{th} equivalent convection heat transfer coefficient of 17 W/(m² C) value was used to verify the wire temperature, which is a typical coefficient for this setup [27]. One must also realize that the resistance of the wire is temperature dependent and can increase by around 30% for wires under the hood compared to wires routed in the cab (which operate at around 20C). To capture this effect the design for both vehicles used the resistance of copper at the worst-case operating temperature of 100C, because most of the wires in the vehicle that transmit power are routed under the hood into the fuse box.

Electromagnetic interference must also be considered when selecting the proper electrical components for the vehicle. The team found many issues with the CAN bus in which the root cause was the lack of shielding, and long wire lengths. Several types of commercially available CAN wire include two insulated conductors surrounded by a shield wire which can be grounded to prevent EMI from causing CAN bus failures.

4.5.3 Low Voltage Wire Preparations

The manner in which electrical connections are made is vital for having a functional and road worthy vehicle. Almost all the components that were integrated in the TVP utilize different style connectors that typically have crimp on pins that get inserted into a plastic connector housing. All the components in the rear battery enclosure were wired into the vehicle via multiple 14 or 4 pin Amphenol circular connectors. These allow the team to disconnect the whole battery box along with individual components, which is important during testing and debugging phases. Rather than having separate power and ground wires for all components, a 2 AWG power and ground cable was ran to the rear of the box, which then terminates to a stud style junction block. All the power and ground pins of the individual components get connected to these junction blocks via a crimp on ring terminal.

Modifications and additions in the electrical system often require the need to connect two separate wires together, as it is usually advantageous to do this rather than route and integrate a completely new wire. This can also be beneficial for extending the life of the delicate electrical connectors, as some of the component's connectors are expensive, fragile, and have long lead times for replacements. There are several processes for this, such as crimp on butt splices, soldering, and crimping on a removeable connector. The fastest option is utilizing a common crimp on butt splice, but often is not a secure connection if not done correctly due to the vibrations that occur when driving, though this can be mitigated with proper cable management. Having the correct set of ratcheting crimpers also helps achieve a better connection, as many of the off the shelf multi tools that crimp and strip do not produce a satisfactory connection and are more difficult to use as they require more strength. The main downfall of crimping in a

university setting is the lack of knowledge and experience within the team about how to properly crimp a connector.

Soldering is much more forgiving in terms of experience level, where an improper crimp will often fail. Soldering takes longer than crimping, and can be difficult to perform in some locations, but typically results in a better connection. Soldering is not a perfect connection, as it is still susceptible to cracking from the vehicle's vibration, but this can also be mitigated like crimping. Soldering can also create a better electrical connection, which may be required for signal or CAN wires. NASA guidance on workmanship and standards for crimping and lap/lineman splice soldering were followed and used as a guide for both vehicles to ensure proper connections [28].

4.6 Powertrain

The integration of the Magna eRAD into the Blazer was simple in comparison to past EcoCAR vehicles that CSU VIT has built, where the manufacturing and installation of the powertrain had to be done with much more care and precision [20]. This stems from the differences in architectures, and that the Blazer's electric motor does not directly interface with the engine. The mounts (shown in green in the figure below) were made from a sheet of steel that was cut on a water jet machine and bent into shape with a metal brake, that was then bolted to the eRAD and rear subframe. The tolerances involved in this process were very loose compared to the TVP powertrain, as any misalignment was easily taken up by the interface of the motor and half shafts.



Figure 20: Blazer rear subframe with Magna eRAD installed

The TVP has a much more complex powertrain, as the YASA P400 motor has a through shaft that directly integrates onto the output of the transmission. The splines on the motor and transmission require tight tolerances to ensure the unit does not have a premature failure. This also means that the motor must not move relative to the transmission during use, and thus the team created a mounting system that is welded to the end of the transmissions tailstock. This mounting system is comprised of two separate aluminum parts that allow the motor to be mounted to the transmission. This setup also requires a custom spline shaft adapter, as the splines of the transmission are not the same as that on the electric motor. These considerations added significant time and effort to the integration of the motor when compared to a P4 system, such as the Blazer.



Figure 21: YASA P400 Installed on the Tacoma Transmission (left) and Transmission/ EM System Installed on Vehicle (right)



Figure 22: Electric motor, transmission, and propulsion shaft installed in vehicle

4.7 Control System Integration

The control systems for both cars utilized a Motohawk HSC for the controller but had different methods of controlling the car. The team had more access to the Blazer's stock control system and could simply send the vehicle CAN messages to control the steering and acceleration

of the vehicle. The TVP however does not have this luxury and must spoof the accelerator pedal position to request a specific torque from the engine. This process was also complicated because the pedal percentage to engine torque maps were not provided to the team. The maps were generated by the team via extensive on road testing of the stock vehicle. Controlling the electric side of the powertrain for each vehicle was essentially identical and was achieved via sending CAN signals to the various controllers on the added CAN bus. The two HSCs also controlled the power to the relays which activated the pumps and fans in the cooling loop, which do not have speed controllers and are either on or off.

4.8 Human Machine Interface

Interfacing and controlling a vehicle is essential for basic functionality as well as for activating more advanced options such as the various modes of vehicle control. The EcoCAR Mobility Challenge had a large focus on consumer usability and driver vehicle interactions. This is due to the nature of the competition and how the teams were essentially building a prototype vehicle for rental applications, and thus it was assumed that the end users would have little to no knowledge on how the vehicle's features worked. Driver educational and intuitive controls for the advanced driver assistance features are critical for safe utilization of these features in the EcoCAR design. The Blazer has several devices that communicate with the driver and receive feedback from the driver to select and input. Four LEDs and switches were mounted on the interior's ceiling, near the stock controls for the moon roof. These switches and feedback LEDs controlled the driver assistance features of the vehicle, and give warnings on this system.

The Blazer also has haptic feedback motors and drivers integrated into the seat belt of the vehicle. This acts as another level of interaction between the car and driver, as it can notify the driver when they are drifting out of the lane, or if they are going to hit something. This module was 3D printed, and enclosed two drivers and haptic vibration motors that were powerful enough to feel through multiple layers of clothing. The placement of the unit is modular, and was designed to be adjustable, as one of the main goals for this prototype was to determine the most optimal position for the permanent integration of the unit that would work best for the largest amount of users. This experimental design was also going to be tested as a warning for several different features to determine which was the most intuitive for the driver. The Figure 23 and 24 below shows the physical 3D printed prototypes as well as the CAD models.

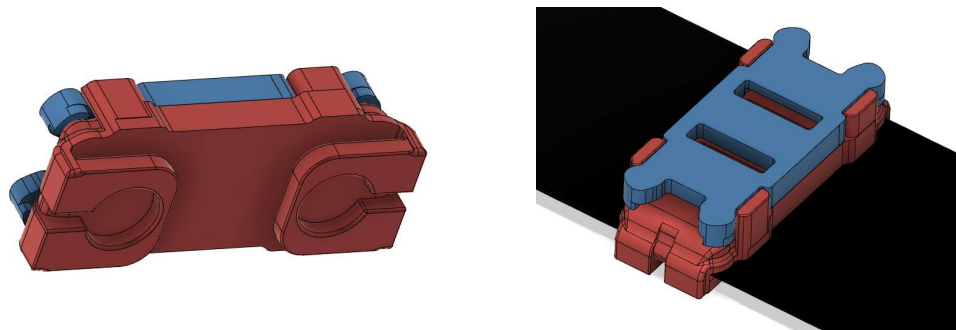


Figure 23: CAD Model of Prototype Haptic Feedback System Housing Bottom view (left) and Top View (right) With Mockup Seat Belt Shown in Black



Figure 24: Haptic feedback system shown installed on the seatbelt with the top view (left) showing the connecting wires and the bottom view (right) showing the haptic motors

The TVP also has numerous controls and displays that are important features for achieving the research goals of the project. On the top of the dash, CSU VIT installed three switches. Two of these switches are simple on/ off signal switches which allows the HSC to know what driving/ PAE mode the vehicles should be in. The third switch on the dash is an auxiliary power switch, which powers the CAN gateway. The emergency disconnect switch is also installed next to these switches in an accessible position of the driver. The BMS also has a CAN controlled gauge that displays several different metrics about the battery, with the main one being SOC. Unfortunately, after many days of troubleshooting CAN bus errors, the team found the source of error was in fact this gauge and thus has been disconnected from the CAN bus until a new unit is installed. This gauge is bolted into a 3D printed housing that is surmounted to the top of the dash, with an interference fit rear cover. This is shown below in Figure 25.



Figure 25: CAD model of the battery gauge (left) and 3D printed part with the battery gauge installed on the dashboard along with the PAE switches, EDS, and gateway power switch(right)

The second set of switches are located in the center channel, on top of the transmission tunnel, and include the controls for the contactors as well as a cup holder. It is often advantageous and quicker for testing and troubleshooting to be able to close the contactors via a manual switch rather than having to connect to the CAN bus or the RS232 port on the BMS. This also allowed this vehicle to continue testing while the BMS replacement was being manufactured and shipped to the team, as the first BMS the team had lost contactor control functionality during a minor thermal event inside the unit when the negative contactor failed. Figure 26 shows the physical implementation and the CAD model of the part.



Figure 26: Contactor control switches CAD model mount (left) and 3D printed part installed in the vehicle

4.9 Cooling System

Many automotive grade EMs and inverter/controllers on the market today are liquid cooled, so having to add another cooling system to the vehicle is something that neither vehicle could avoid. The addition of another cooling system requires special design considerations, as it is advantageous from a heat transfer perspective to not have air pockets or bubbles in the system, as this lowers the thermal capacity of the coolant. Careful consideration for component placement in the cooling loop must be taken to minimize these effects. This usually means having the reservoir be the highest point in the system, which can be challenging from a space claim and integration perspective.

Figure 27 shows the thermal loop for the Blazer, which includes the engines cooling system, the added intercooler, as well as the second coolant loop in the rear of the vehicle responsible for keeping the motor and inverter within their respective operating temperatures.

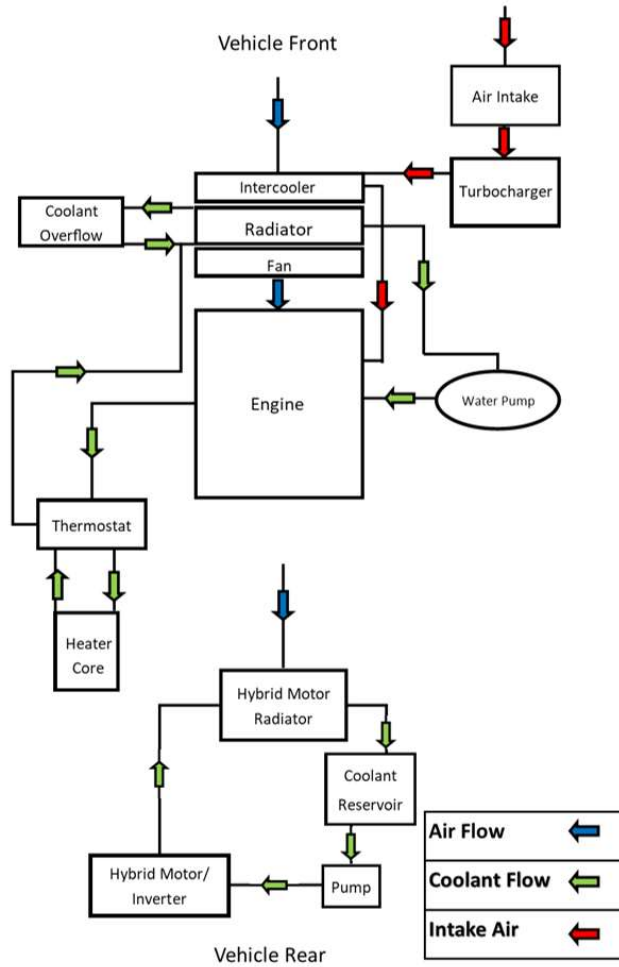


Figure 27: Blazer cooling loop diagram

For the combustion engine cooling system, the high point of the cooling loop is located at the fill cap and neck. This is done to help air bleed out of the system. The low point of the

system is the bottom radiator outlet, which is used as the drain point in the event of service being necessary.

The radiator for the LTG cooling system utilizes the OEM Blazer radiator. Using the stock radiator and position allows for the original coolant temperature bounds, and low coolant level sensors to be used. Due to limited space in the engine bay the turbocharger's intercooler was placed in front of the engine radiator.

The TVP does not utilize an aftermarket intercooler for the engine but does have complexities of its own in the thermal system. The YASA P400 utilizes a special dielectric fluid for cooling the internal components of the motor, which is drastically different than the antifreeze (AF) used for the high voltage charger and motor controller. This requires a second cooling loop to be installed to separate these two fluids. The team decided to use a liquid-to-liquid heat exchanger rather than adding another radiator to the front of the vehicle. This liquid-to-liquid heat exchanger allows the YASA cooling loop to dump its heat into the antifreeze loop, which then can shed this excess heat as it goes through the radiator located at the front of the car. The main reason the team decided to use the liquid-to-liquid heat exchange was to prevent further blocking of the ICE's stock radiator, as the team has limited knowledge of the specifications of this component.

All the components in the TVP's coolant system besides the front radiator were mounted on custom brackets made from welded mounts that were bolted to the bed of the vehicle. These mounts have a large factor of safety for the parts being carried when under the specified load that is industry standard (8 Gs lateral and front to back, 20 Gs vertical). With this load, assuming the worst-case scenario with a simple cantilever beam the max deflection can be found with Equation 12 below, where P is the distributed load, L is the length, E is the modulus, and I is the

moment of inertia of the angle iron [29] [30]. Given the yield strength of the material [31] [32], dimensions, and load the material part would have a safety factor of around 5.5 for yielding.

$$\delta_{max} = \frac{P * L^4}{8 * E * I} \quad \text{Equation 12}$$



Figure 28: TVP antifreeze reservoir mount with battery box rear mounting holes shown

Chapter 5: Fabrication Methodology

One of the main concerns when fabricating and integrating a complex system is manufacturability, which can be a challenge due to lack of experience with many student run programs. The team's knowledge and experience with fabrication methods must be known prior to designing and planning a build with as many complex components as each of the vehicles contain. All but one of the parts that were welded were done in house, which saved the team time and money and allowed for design changes that could be executed in a day or two rather than weeks and months. Several parts were 3D printed, which also saved the team an immense amount of time and money. With an experienced team member and a cheap on hand printer the fabrication time for a 3D printed part is less than what it would take to go to a hardware store and purchase fabrication materials. This is ideal for small cosmetic parts, or mounts that hold noncritical and light weight parts, such as the mount of the CAN gateway shown below in Figure 29. This is due to a variety of factors specific to fused filament fabrication which can lead to uncertainties in performance, as well as the complexities in generating accurate FEA models for this fabrication process [33] [34].



Figure 29: CAN gateway mount CAD (left) and 3D printed part with the gateway installed (right)

This however is not to say that new and experimental processes cannot be utilized by the team. For example, the clearance hole in the transmission tunnel for the motor needed a cover to prevent road debris from entering the cab. The team simply took an extra piece of acrylic and used a heat gun to bend the cut part into the complex 3D shape of the hole (shown in Figure 30 below). However, this part is not structural so if the inexperience of the team leads to a bad part it is not an issue, unlike many of the welded parts.



Figure 30: Transmission tunnel hole with acrylic cover

Chapter 6: Testing and Results

Before any testing with the vehicle was done several safety tests were performed. The first set of tests were focused on emergency system shut downs, and ensured that the safety of the team members would not be jeopardized in an emergency. These tests were performed early in the integration process before any high voltage or low voltage components were plugged in. This was simply performed by measuring voltage on the power pins of all connectors on the wiring harness with the EDS pressed and depressed. This test was repeated often during integration, especially after any wiring or system changes. The team then checked the high voltage isolation, testing the resistance between the high voltage system and low voltage system as well as the stock vehicles chassis ground. The industry standard resistance is 500 ohms per volt, and the team measured approximately 10 mega ohms, which is well within this industry standard for the TVP's HV system.

The HV battery was then put through its paces with charge testing, as well as zero velocity on lift tests to ensure the battery was discharging properly. During initial charging, the team found several cells which were not receiving a charge, but also had no signs of damage when analyzing temperature and internal resistance. The cells were removed from the pack and replaced with new cells along with new cell sensor boards. Figure 31 below shows how the battery current and voltage remains in the proper operating range during discharge. Average battery cell temperature was also logged during the tests, and it was found that it increased by two degrees over the first 5 minutes of testing, and then remained constant during the remaining duration of the test. This zero-velocity lift test also confirmed the software did not have any bugs that could damage any components and that the vehicle's control system was working properly.

This test however did have to be kept to wheel speeds of under 10 miles per hour, as the vehicles traction control would engage and hinder the team’s ability to accurately control the engine.

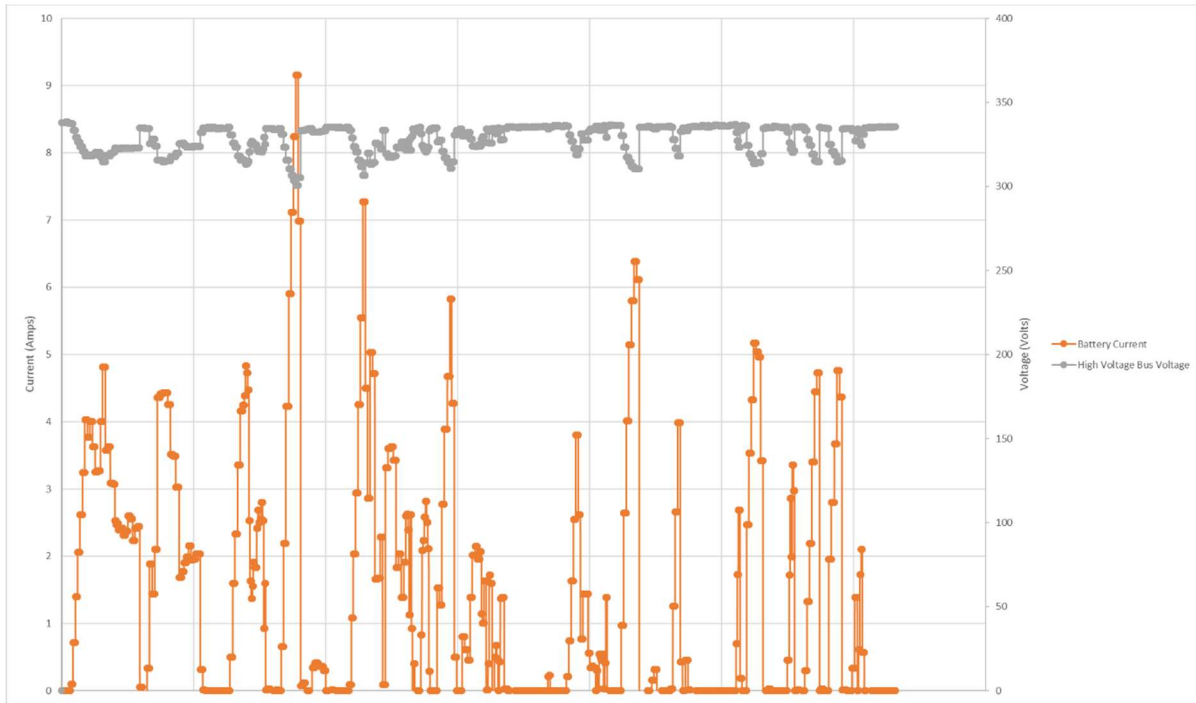


Figure 31: High voltage DC bus current and voltage

Once the on lift zero velocity testing was completed without issues, the team then moved onto to test the vehicle’s hybrid capability on the open road. Before any testing of new software and or hardware configurations the team ensured the vehicle was safe to drive on the road and operating as intended by driving the vehicle around the garage parking lot before venturing out onto public roads. The first open road test run was a simple validation of the hybrid system at speeds greater than the 10 mph the zero-velocity lift testing was capable of. For this a manual torque split was set, where 10% of the driver requested torque came from the electric motor, and 90% came from the ICE. The electric motor was also capped at a maximum torque of 15 Nm for

the first few runs. The purpose of this test was to ensure that the powertrain and control system was working as intended and no issues arise when driving under hybrid power at higher speeds. Figure 32 below depicts the engine torque and electric motor torque over a single drive cycle. This confirms that the powertrain torque commands are working as intended and the control system of the vehicle is fully functional. With the gain in confidence, the team then increased the torque split to 70% ICE and 30% EM and tested the powertrain again, to further verify the electric motor is indeed providing the torque that is being commanded, which can be seen in Figure 33.

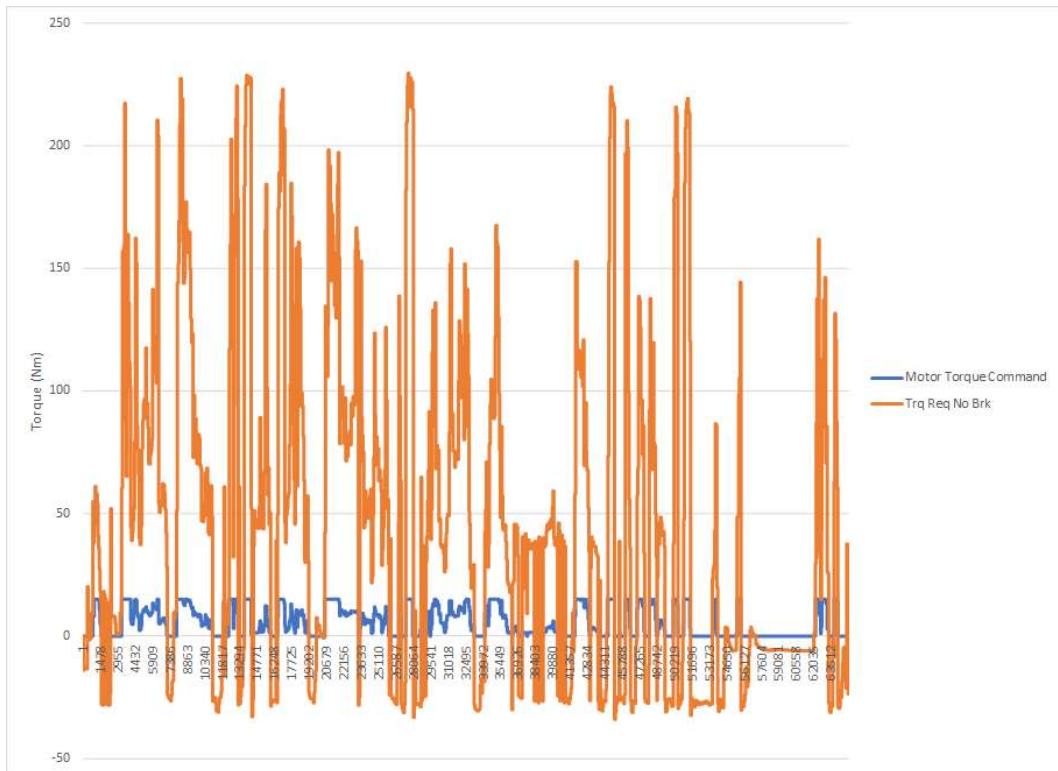


Figure 32: Engine and electric motor torque for 90% ICE 10% EM torque split

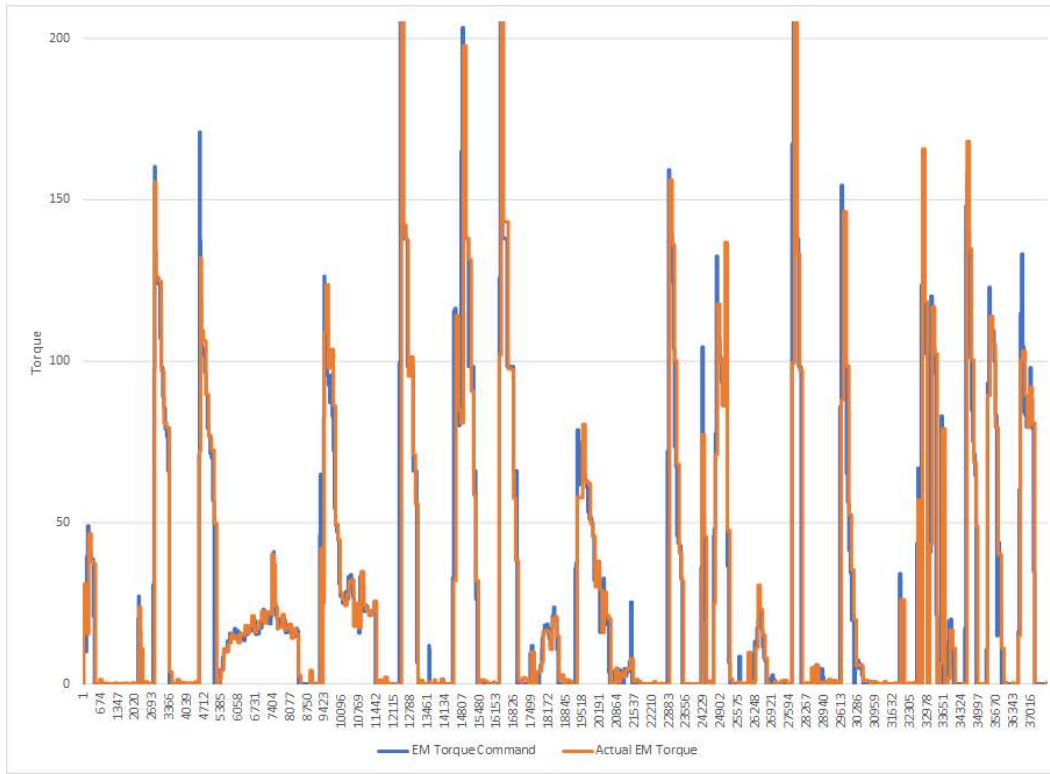


Figure 33: Torque commanded and actual torque from the electric motor

During initial testing, a thermocouple was installed on the high voltage wires at the closest point to the exhaust. The purpose of this test was to confirm that the heat shielding installed by the team would be sufficient protection from the high temperature present near engine exhaust components which would be the highest temperature the wires would be exposed to. The following figure is a plot of the temperature of the wires during testing which confirms the high voltage wires are well within operating temperatures and the wire’s heat shielding is sufficient.

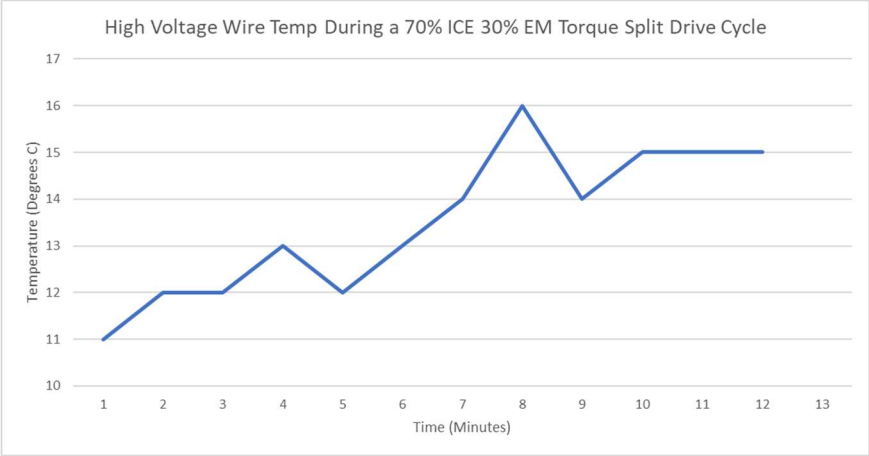


Figure 34: High voltage wire temperature

Chapter 7: Discussion

The result of the integration of the hybrid system of the TVP was successful, showing via testing that the vehicle is capable of accomplishing the research goals, as all of the added components necessary for the integration of a P3 parallel hybrid are fully functional despite the numerous hurdles the team had to overcome. The vehicle has all the necessary controls hardware, hybrid components, and data acquisition methods to be a successful platform to test hybrid vehicle control strategies for not only PAE, but future projects. The flexibility to make changes to the vehicles parameters and control software make this an ideal platform for testing new controls strategies. The component integration and wiring are also somewhat future proofed, with extra power and signal wires in many locations on the vehicle, such as the glovebox, battery box, and front bumper. This will allow for the integration of new features and components onto the vehicle to further mature the performance of the vehicles controls strategy beyond what the scope of the initial research goals contain.

Several prototype vehicles in the past have integrated hybrid systems into traditional ICE vehicles, each with differing research goals [20] [35] [36]. In contrast, the TVP is the first documented vehicle that incorporates a predictive optimal energy management control-enabled hybrid vehicle. The TVP can be utilized to demonstrate real world gains in FE that can in turn, have a widespread impact on new hybrid vehicles and the controls development of these systems.

Chapter 8: Conclusion

The hybrid vehicle systems that have been discussed in this paper will be used to further test PAE based controls as well as other controls schemes. This will also serve as a test platform for future vehicle projects. The intimate details within this paper will aid in the understanding of the overall scope and vision for the projects, as well as the limitations.

This thesis has outlined the purpose, scope, and vision of the two vehicles CSU VIT has constructed. These over arching themes then were distilled down into several design requirements, each of which were unique to the respective vehicles, and led to major differences in design that have been compared in this paper. These design requirements then led the component selection process, where each of the major systems in the vehicle had an explanation of the reasons behind the selection of each component. This process drove the design and integration procedure for the installation and verification of all the added components the team selected. During this process the fabrication methodology for each system was analyzed. Finally, the system testing processes and results were presented. This showed the full functionality of the hybrid powertrain system, as well as its capability to accurately generate results for the research questions proposed. This work also presented the flexibility of the controls system and how the team can quickly manipulate and test the vehicle to ensure that it is functioning as intended and that the performance goals were met in a safe and timely manner.

Future work on the TVP would include an in-depth analysis on the CAN bus noise. The team has pinpointed the root cause of the issue to be the high voltage system, as the CAN bus gets significantly noisier when the contactors are closed. The vehicle is at a point in which the

control system still runs with the installed CAN bus but will still occasionally display minor errors. Several mitigation techniques for reducing the errors have been integrated into the vehicle. This allowed the CAN bus to be fully functional, however it still does have some of these errors present and future work could address these issues.

The BMS functionality is another area that future students could focus on. Often during testing, the team would activate the hybrid system and the high voltage contactors would close, the BMS would fault as it loses communication with several battery banks, which opens contactors as the unit faults out. This error is seemingly random and has no specific pattern to when it will occur. A deep dive into the BMS's inner workings and configuration settings could allow the team to avoid having to power cycle the system when this issue occurs. The team briefly explored different procedures and timings of powering on the BMS and inverter, enabling the inverter, and closing contactors. However, this work did not resolve the issue as the process that was found to resolve the issue is a power cycle of the BMS.

References

- [1] U.S. Energy Information Administration , "U.S. energy-related CO2 emissions rose in 2018 for the first year since 2014," *Independent Statistics and Analysis*, 2019.
- [2] K. Desmet and E. Rossi-Hansberg, "On the spatial economic impact of global warming," *Journal of Urban Economics*, vol. 88, pp. 16-37, 2015.
- [3] A. Singh and P. Bharathi, "Public Health Impacts of Global Warming and Climate Change," *Peace Review*, vol. 26, pp. 112-120, 2014.
- [4] M. Fritz, P. Plotz and S. Funke, "The impact of ambitious fuel economy standards on the market uptake of electric vehicles and specific CO2 emissions," *Energy Policy*, vol. 135, p. 111006, 2019.
- [5] United States Environmental Protection Agency , "Public Review of Draft U.S. Inventory of Greenhouse Gas Emissions and Sinks: 1990-2019," 2019.
- [6] J. Whitehead, J. P. Franklin and S. Washington, "Transitioning to energy efficient vehicles: An analysis of the potential rebound effects and subsequent impact upon emissions," *Transportation Research Part A: Policy and Practice*, vol. 74, pp. 250-267, 2015.
- [7] D. A. Trinko, *Predictive Energy Management Strategies for Hybrid Electric Vehicles Applied During Acceleration Events*, Fort Collins, Co: Colorado State University , 2019.
- [8] P. S. A. R. S. Pagerit, "Fuel Economy Sensitivity to Vehicle Mass for Advanced Vehicle Powertrains," *SAE Technical Paper*, p. 19, 2006.
- [9] S. M. Lukic and E. Emadi, "Effects of drivetrain hybridization on fuel economy and dynamic performance of parallel hybrid electric vehicles," *IEEE Transactions on Vehicular Technology*, vol. 53, no. 2, pp. 385-389, 2004.
- [10] M. R. Cuddy and K. B. Wipke, "Analysis of the Fuel Economy Benefit of Drivetrain Hybridization," *SAE Transactions*, vol. 106, no. 6, pp. 475-485, 1997.
- [11] V. H. Johnson, K. B. Wipke and D. J. Rausen, "HEV Control Strategy for Real-Time Optimization of Fuel Economy and Emissions," *SAE Technical Paper*, p. 16, 2001.
- [12] P. Pisu and G. Rizzoni, "A Comparative Study Of Supervisory Control Strategies for Hybrid Electric Vehicles," *IEEE Transactions on Control Systems Technology*, vol. 15, no. 3, pp. 506-518, 2007.
- [13] K. Kerem, "Modeling and Control of a Hybrid-Electric Vehicle for Drivability and Fuel Economy Improvements," Ohio State University, 2008.
- [14] N. A. Khier, M. A. Salman and N. J. Schouten, "Emissions and fuel economy trade-off for hybrid vehicles using fuzzy logic," *Mathematics and Computers in Simulation*, vol. 66, no. 2-3, pp. 155-172, 2004.

- [15] Z. D. Asher, D. A. Trinko and T. H. Bradley, "Increasing the Fuel Economy of Connected and Autonomous Lithium-Ion Electrified Vehicles," in *Behaviour of Lithium-Ion Batteries in Electric Vehicles*, Springer, 2018, pp. 129-151.
- [16] D. A. Trinko, Z. D. Asher and T. H. Bradley, "Application of Pre-Computed Acceleration Event Control to Improve Fuel Economy in Hybrid Electric Vehicles," *SAE Technical Paper*, p. 7, 2018.
- [17] Z. Asher, D. Trinko, J. Payne, B. Geller and T. Bradley, "Real-Time Implementation of Optimal Energy Management in Hybrid Electric Vehicles: Globally Optimal Control of Acceleration Events," *Journal of Dynamic Systems, Measurement, and Control*, vol. 142, no. 8, p. 19, 2020.
- [18] "Autonomie.net," About Landing Page, 2021. [Online].
- [19] Z. Asher, J. Tunnell, D. Baker, R. Fitzgerald, F. Banaei-Kashani, S. Pasricha and T. Bradley, "Enabling Prediction for Optimal Fuel Economy Vehicle Control," *SAE Technical Paper*, 2018.
- [20] D. Gabe, J. Bair, J. Tunnell and et al., "Colorado State University EcoCAR 3 Final Technical Report," *SAE Technical Papers*, p. 15, 2019.
- [21] M. Ozguc, E. Ipek, K. Aras and K. Erhan, "Comprehensive Analysis of Pre-Charge Sequence in," *TRANSACTIONS ON ENVIRONMENT AND ELECTRICAL ENGINEERING*, vol. 4, no. 1, 2020.
- [22] "Charging Lithium-ion," Battery University, 24 04 2018. [Online]. Available: https://batteryuniversity.com/learn/article/charging_lithium_ion_batteries. [Accessed 18 04 2021].
- [23] "Li-ion Lithium Ion Battery Charging," Electronics Notes, 2014. [Online]. Available: https://www.electronics-notes.com/articles/electronic_components/battery-technology/li-ion-lithium-ion-charging.php. [Accessed 2021].
- [24] S. International, "SAE Electric Vehicle and Plug in Hybrid Electric Vehicle Conductive Charge Coupler".
- [25] L. H. Sargent, "ECOCAR 3 INTERCONNECT DEFINITIONS, DESCRIPTIONS AND JUSTIFICATIONS," vol. 1, p. 45, 2017.
- [26] F. P. Incropera, D. P. Dewitt, T. L. Bergman and A. S. Lavine, *Principles of Heat and Mass Transfer*, Wiley, 2014.
- [27] T. Bradley, *HV Electrical Systems for Vehicles*, Fort Collins, CO: Colorado State University, 2017.
- [28] National Aeronautics and Space Administration, "WORKMANSHIP STANDARD FOR CRIMPING, INTERCONNECTING CABLE, HARNESS, AND WIRING," Vols. NASA-STD 8739.4A, 2016.
- [29] R. C. Hibbeler, *Mechanics of Materials*, 9th Edition: Pearson, 2015.
- [30] R. G. Budynas and K. J. Nisbett, *Shigley's Mechanical Engineering Design*, McGraw Hill, 2016.

- [31] "Engineering Tool Box: Young's Modulus," [Online]. Available: https://www.engineeringtoolbox.com/young-modulus-d_417.html. [Accessed 17 4 2021].
- [32] J. S, "Plain Carbon Steels: Classification and Limitations | Metallurgy," [Online]. Available: <https://www.engineeringenotes.com/metallurgy/steel/plain-carbon-steels-classification-and-limitations-metallurgy/25621>. [Accessed 17 4 2021].
- [33] G. Grob, "FEA and 3D printing – challenges and potential workarounds," *GrabCAD*, 17 4 2016. [Online]. Available: <https://blog.grabcad.com/blog/2016/04/27/fea-and-3d-printing-challenges/>. [Accessed 2021].
- [34] M. Molitch-Hou, "FEA Analysis and Predicting the Performance of 3D Printing," *Engineering.com*, 17 11 2016. [Online]. Available: <https://www.engineering.com/story/story/fea-analysis-and-predicting-the-performance-of-3d-printing>. [Accessed 2021].
- [35] F. L. Mapelli, D. Tarsitano and M. Mauri, "Plug-In Hybrid Electric Vehicle: Modeling, Prototype Realization, and Inverter Losses Reduction Analysis," *IEEE Transactions on Industrial Electronics*, vol. 57, no. 2, 2010.
- [36] M. Carello, N. Filippo and R. D'Ippolito, "Performance Optimization for the XAM Hybrid Electric Vehicle Prototype," *SAE Technical Papers*, p. 12, 2012.
- [37] D. Trinko, Z. Asher and T. Bradley, "Application of Pre-Computed Acceleration Event Control to Improve Fuel Economy in Hybrid Electric Vehicles," *Society of Automotive Engineers Technical Papers*, p. 7, 2018.

Appendix

Pre-Charge Resistor Calculation MATLAB Script

```
% PreCharge Resistor Calculation
format long; clear all, close all; clc
%% Input params
PCT = 1.5;% (Sec) Desired precharge time
C = .0009;% (Farads) Capacitance across HV DC in for inverter
Vb = 345;% (Volts) Battery voltage

%% Resistance calculation
Tau = PCT/5;% () RC constant of circuit (5 tau used for charge)
disp('Resistance value needed (Ohms)')
R = Tau/C % (Ohms) Resistor value needed

%% Resistance rating calculation
E = (C*Vb^2)/2;% (joules) Energy dissipated by the resistor
disp('Power rating needed for resistor (Watts)')
P = E/PCT % (Watts)Max power through resistor

%% Voltage and Current profiles over time
T = [0:0.0001:PCT];

% The following R can be used to override the prescribed R value.
% Notice the current spike if you lower this resistance to a smaller value
% that is more typical of just a wire, which simulates no resistor
% R below was measured from Battery to inverter W/O the PC Resistor
R = 0.15; (ohms)
Vc = Vb*(1-exp(-T/(R*C))); % (Volts) Voltage on the capacitor
Ic = (Vb-Vc)/R; % (Amps) Inrush current over time
Pc = (Ic.^2)*R/1000 ;% (Watts) Power in cap over time

%% Plot the results

yyaxis left
xlabel('Time (Seconds)')

title('Inrush Voltage and Current')
plot(T, Vc);
ylabel('Inrush Voltage (Volts)')
hold on;
yyaxis right
ylabel('Inrush Current (Amps)')
plot(T,Ic);
```

```

hold off
figure
plot(T, Pc)
title('Power')
xlabel('Time (Seconds)')
ylabel('Power (Watts)')

```

Battery Management System Parameters

Tab in GUI	Parameter	Value (units provided in GUI)
Basic	Capacity	40
Cell-V	V max	3.7
Cell-V	V high	3.65
Cell-V	V low	3.0
Cell-V	V min	2.65
Measure	Source current sensor gain	150
Measure	Source current sensor offset	4104
Measure	Load current sensor gain	50
Measure	Load current sensor offset	4092
Protect	Peak current	120
Protect	Cont current	40
Protect	Max temp	60
Protect	Min temp	0
Balance	Min balance cell voltage	3.2
Balance	Min delta in cell voltage	50
Control	Min precharge time	1.5

List of Abbreviations

AC: Alternating Current
AF: Antifreeze
APM: Auxiliary Power Module
AVTC: Advanced Vehicle Technology Competition
AWG: American Wire Gauge
BEV: Battery Electric Vehicle
BMS: Battery Management System
CAD: Computer Aided Design
CAN: Controller Area Network
CAV: Connected and Automated Vehicles
DC: Direct Current
DOE: Department of Energy
ECM: Engine Control Module
EM: Electric Motor
EMC: Electric Motor Controller
EMI: Electromagnetic Interference
eRAD: Electrified Rear Axle Drive
EVSE: Electric Vehicle Supply Equipment
FE: Fuel Economy
FEA: Finite Element Analysis
GM: General Motors
GUI: Graphical User Interface
HEV: Hybrid Electric Vehicle
HSC: Hybrid Supervisory Controller
HVJB: High Voltage Junction Box
ICE: Internal Combustion Engine

IP: Ingress Protection

MSD: Manual Service Disconnect

NEMA: National Electrical Manufacturers Association

OBC: Onboard Charger

OEM: Original Equipment Manufacturer

PAE: Predictive Acceleration Events

PCB: Printed Circuit Board

PWM: Pulse Width Modulation

RDM: Rear Drive Module

RMS: Rinehart Motion System

SOC: State of Charge

TCM: Transmission Control Module

TVP: Test Vehicle Platform

VIT: Vehicle Innovation Team